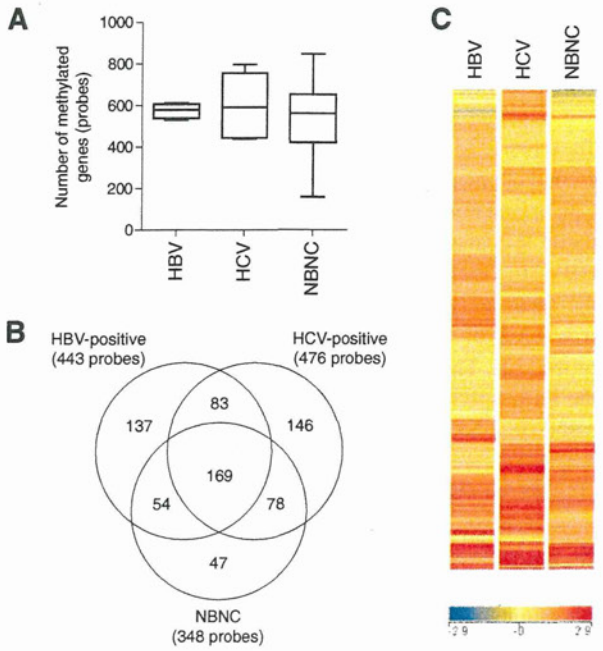

Fig. 1 Genome-wide analysis of CpG island methylation. **a** MCAM analysis was carried out using a series of HCC tissue specimens (HBV-positive, $n=4$; HCV-positive, $n=5$; HBV/HCV-negative, NBNC, $n=7$). MCAM data were categorized into three groups based on the hepatitis virus status, and the numbers of methylated genes in the respective categories are shown. **b** Venn diagram analysis of the methylated genes in the indicated categories. **c** Gene tree view of the MCAM analysis results. A set of 714 probes (514 unique genes) were selected as commonly methylated genes, after which, hierarchical clustering was performed. Each row represents a single probe

number were commonly methylated in HCC. Because recent studies have suggested that aberrant DNA methylation could be a useful diagnostic marker for HCC, we next aimed to identify novel genes frequently methylated in HCC. Among the genes commonly methylated irrespective of hepatitis virus status, we selected 14 (*KLHL35*, *PAX5*, *PENK*, *SPDYA*, *LTBP2*, *DLX1*, *PGBD1*, *WNT9A*, *ADRA1A*, *RHOBTB1*, *GDNF*, *WNT11*, *MLL*, and *PLEC1*) and carried out MSP to assess their methylation status in a series of HCC cell lines (Supplementary Fig. 3). We found that four (*KLHL35*, *PAX5*, *PENK*, and *SPDYA*) of the genes were frequently methylated in HCC cell lines, but showed only little or no methylation in normal liver tissue from a healthy individual (Supplementary Fig. 3). We therefore used quantitative bisulfite pyrosequencing to further analyze the methylation levels of these four genes (Supplementary Figs. 4 and 5).

To determine the extent to which these genes are aberrantly methylated in primary tumors, we analyzed a set of primary HCC specimens (HBV-positive, $n=21$; HCV-positive, $n=21$; HBV/HCV-negative, $n=15$) and corresponding noncancerous liver tissues from the same patients (HBV-positive, $n=18$; HCV-positive, $n=18$; HBV/HCV-negative, $n=14$). Bisulfite pyrosequencing analysis revealed the methylation levels of the four genes to be significantly higher in tumor tissues than in their noncancerous counterparts (*KLHL35*, 37.9 vs. 10.4 %, $P<0.001$; *PAX5*, 23.4 vs. 7.7 %, $P<0.001$; *PENK* 41.1 vs. 22.0 %, $P<0.001$; *SPDYA*, 49.7 vs. 19.3 %, $P<0.001$) (Supplementary Fig. 6). Moreover, these genes were frequently methylated in HCCs, irrespective of the hepatitis virus infection (*KLHL35*, HBV-positive, 37.5 vs. 9.9 %, $P<0.001$; HCV-positive, 38.3 vs. 9.0 %, $P<0.001$; HBV/HCV-negative, 37.7 vs. 13.0 %, $P<0.001$; *PAX5*, HBV-positive, 22.2 vs. 7.6 %, $P=0.014$; HCV-positive, 26.5 vs. 7.2 %, $P<0.001$; HBV/HCV-negative, 20.7 vs. 8.5 %, $P=0.017$; *PENK*, HBV-positive, 45.1 vs. 20.9 %, $P<0.001$; HCV-positive, 39.2 vs. 23.5 %, $P=0.001$; HBV/HCV-negative, 38.2 vs. 21.3 %, $P=0.006$; *SPDYA*, HBV-positive, 51.5 vs. 19.8 %, $P<0.001$; HCV-positive, 46.6 vs. 15.3 %, $P<0.001$; HBV/HCV-negative, 51.3 vs. 23.7 %, $P<0.001$) (Fig. 2a). The association between the methylation of each gene and the clinicopathological features are shown in Table 1. Methylation of *KLHL35* and *PAX5* was correlated with greater age, and *SPDYA* methylation was moderately correlated with higher PIVKA-II levels, but we found no other significant correlations (Table 1). We also generated an ROC curve and observed that methylation of the four genes discriminated strongly between tumor tissues and noncancerous liver tissue, suggesting that methylation of these genes could be a useful tumor marker (Fig. 2b). The most discriminating cutoffs for *KLHL35*, *PAX5*, *PENK*, and *SPDYA* were 14.8 % (sensitivity, 82.5 %; specificity, 88.0 %), 12.5 % (sensitivity, 63.2 %; specificity, 94.0 %), 28.4 % (sensitivity, 70.2 %; specificity, 96.0 %), and 30.3 % (sensitivity, 86.0 %; specificity, 94.0 %), respectively.

Analysis of *KLHL35*, *PAX5*, *PENK*, and *SPYDA* methylation and expression

We next tested whether methylation of *KLHL35*, *PAX5*, *PENK*, and *SPYDA* was associated with their silencing in HCC. Bisulfite pyrosequencing analysis revealed that the degree to which these genes were methylated varied among the HCC cell lines, but it was always much higher than in normal liver tissue from a healthy individual (Fig. 3a). Quantitative RT-PCR analysis confirmed an inverse relationship between methylation and expression of *KLHL35*

Fig. 2 Quantitative methylation analysis of the genes identified by MCAM. **a** Summary of the bisulfite pyrosequencing analysis of *KLHL35*, *PAX5*, *PENK*, and *SPDYA* in tumor tissue (*T*) and noncancerous liver tissue (*N*) from HBV-positive, HCV-positive, and HBV/HCB-negative (NBNC) HCC patients. **b** ROC curve analysis of the methylation of the indicated genes. The area under the ROC curve (*AUC*) for each site conveys its utility (in terms of sensitivity and specificity) for distinguishing between HCC tissue and corresponding noncancerous liver tissue from the same HCC patients

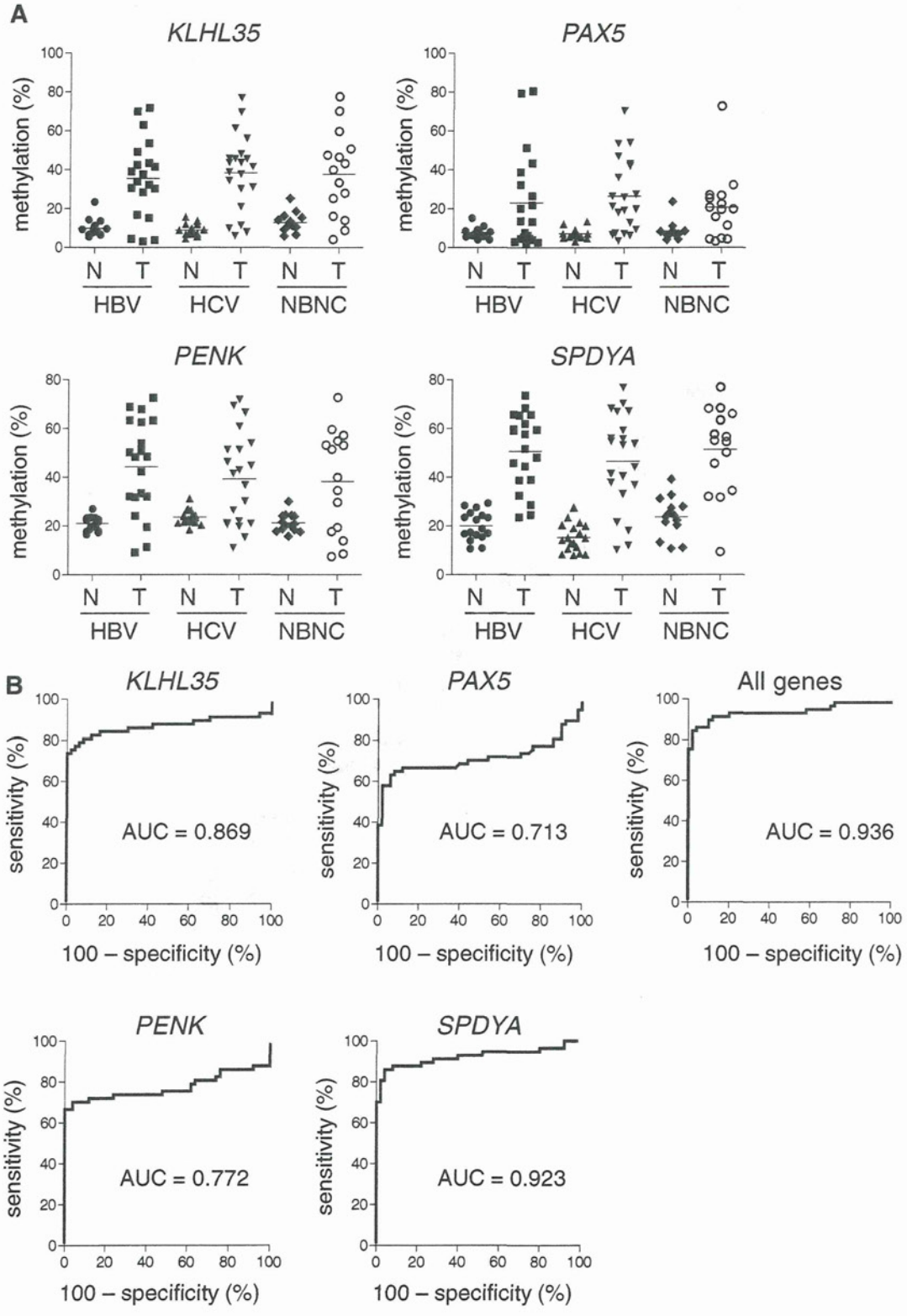

and *PAX5* in the cell lines and normal liver tissue (Fig. 3b), whereas methylation of *PENK* and *SPDYA* did not correlate significantly with their expression levels. The expression of *PENK* was undetectable in seven HCC cell lines and in

t1.1 **Table 1** Association between clinicopathological features and DNA methylation in HCC

t1.2		*N*	*KLHL35* methylation			*PAX5* methylation			*PENK* methylation			*SPDYA* methylation			LINE-1 methylation		
t1.3			Mean	SD	*P* value	Mean	SD	*P* value	Mean	SD	*P* value	Mean	SD	*P* value	Mean	SD	*P* value
t1.4	Age																
t1.5	≤63	24	30.3	17.7	0.003	18.3	17.1	0.026	41.7	19.3	0.583	51.2	17.9	0.945	49.4	14.8	0.571
t1.6	>64	23	47.2	18.5		32.3	24.1		44.8	19.6		50.9	15.0		47.2	10.6	
t1.7	Sex																
t1.8	M	39	37.5	20.3		22.6	20.9		40.2	19.6		50.1	18.1		47.8	13.3	
t1.9	F	18	37.2	22.0	0.953	25.2	19.9	0.652	43.1	19.6	0.602	48.7	16.7	0.771	51.5	12.0	0.318
t1.10	Virus																
t1.11	HBV	21	35.6	20.3		23.1	24.5		44.3	19.4		50.7	15.4		50.4	13.9	
t1.12	HCV	21	38.3	19.5		26.5	19.0		39.2	18.8		46.6	19.6		50.2	12.2	
t1.13	NBNC	15	36.1	22.2	0.900	20.7	17.2	0.698	38.2	21.0	0.603	51.3	18.0	0.668	44.7	12.9	0.359
t1.14	Child-Pugh																
t1.15	A	44	39.2	20.0		25.5	22.3		43.4	19.6		51.4	15.6		48.6	12.4	
t1.16	B	3	29.7	18.2	0.426	19.9	11.8	0.672	41.0	17.1	0.842	45.3	29.5	0.536	44.6	20.6	0.609
t1.17	PIVKA-II (mAU/ml)																
t1.18	≤21	16	40.0	19.5		24.0	25.7		42.1	19.1		53.5	14.1		48.0	11.5	
t1.19	22–66	16	35.8	11.8		23.4	14.2		44.6	14.0		42.9	15.9		52.9	10.7	
t1.20	>67	15	40.1	26.9	0.795	28.3	24.8	0.802	42.8	24.9	0.933	57.1	16.6	0.039	43.8	15.1	0.136
t1.21	AFP (ng/ml)																
t1.22	≤7.4	16	39.3	19.3		25.8	24.1		41.4	19.0		49.4	17.0		47.4	9.2	
t1.23	7.5–55.0	16	44.9	20.2		31.1	23.2		51.5	15.6		55.0	16.7		50.6	13.4	
t1.24	>55.1	15	31.1	18.7	0.150	18.1	16.3	0.256	36.3	21.0	0.078	48.7	15.8	0.509	46.9	15.7	0.695
t1.25	Cirrhosis																
t1.26	0	27	35.3	23.4		22.2	22.2		40.0	22.1		51.8	18.2		47.7	14.7	
t1.27	1	24	40.7	16.5	0.353	25.7	20.3	0.559	44.2	17.8	0.467	50.5	15.8	0.795	49.2	11.3	0.687
t1.28	Vascular invasion																
t1.29	0	42	38.3	18.5		24.0	21.0		43.9	19.5		52.3	15.1		48.2	12.8	
t1.30	1	9	35.7	28.9	0.353	23.1	23.3	0.559	33.1	21.5	0.467	46.1	24.2	0.795	49.3	15.1	0.687
t1.31	TNM stage																
t1.32	1	6	29.5	15.4		15.0	9.8		50.6	12.1		43.3	20.8		58.4	11.8	
t1.33	2	20	37.7	20.4		24.6	20.3		44.7	19.3		53.7	11.8		47.5	13.2	
t1.34	3	13	45.4	14.3		24.4	23.4		43.0	19.3		55.5	13.8		44.8	10.6	
t1.35	4	6	32.4	28.6	0.335	30.9	28.4	0.639	29.4	23.3	0.262	41.6	25.5	0.181	47.5	16.1	0.200
t1.36	Multiple cancer																
t1.37	0	33	38.3	22.1		26.2	23.9		43.9	20.8		51.1	18.5		48.8	14.2	
t1.38	1	13	38.6	14.3	0.964	22.4	16.9	0.609	41.7	16.4	0.732	50.5	10.7	0.911	48.3	8.5	0.916

NBNC HBV/HCV-negative

normal liver tissue, irrespective of the methylation status (Fig. 3b). Conversely, although *SPDYA* was highly methylated in a majority of HCC cell lines, its expression was detectable in all cells, and most of the HCC lines exhibited greater *SPDYA* expression than did normal liver tissue (Fig. 3b). The above results suggest that *KLHL35* and *PAX5* are epigenetically silenced in HCC cells. Consistent with that idea, treating methylated cell lines with a DNA methyltransferase inhibitor, 5-aza-dC, restored the expression of *KLHL35* and *PAX5* (Fig. 3c). On the other hand, the expression of *PENK* and *SPDYA* does not appear to be affected by methylation.

Analysis of LINE-1 methylation and its association with gene hypermethylation

It was previously reported that LINE-1 is frequently hypomethylated in HCC, though most of those studies focused on HBV-positive tumors. Similarly, by using the bisulfite

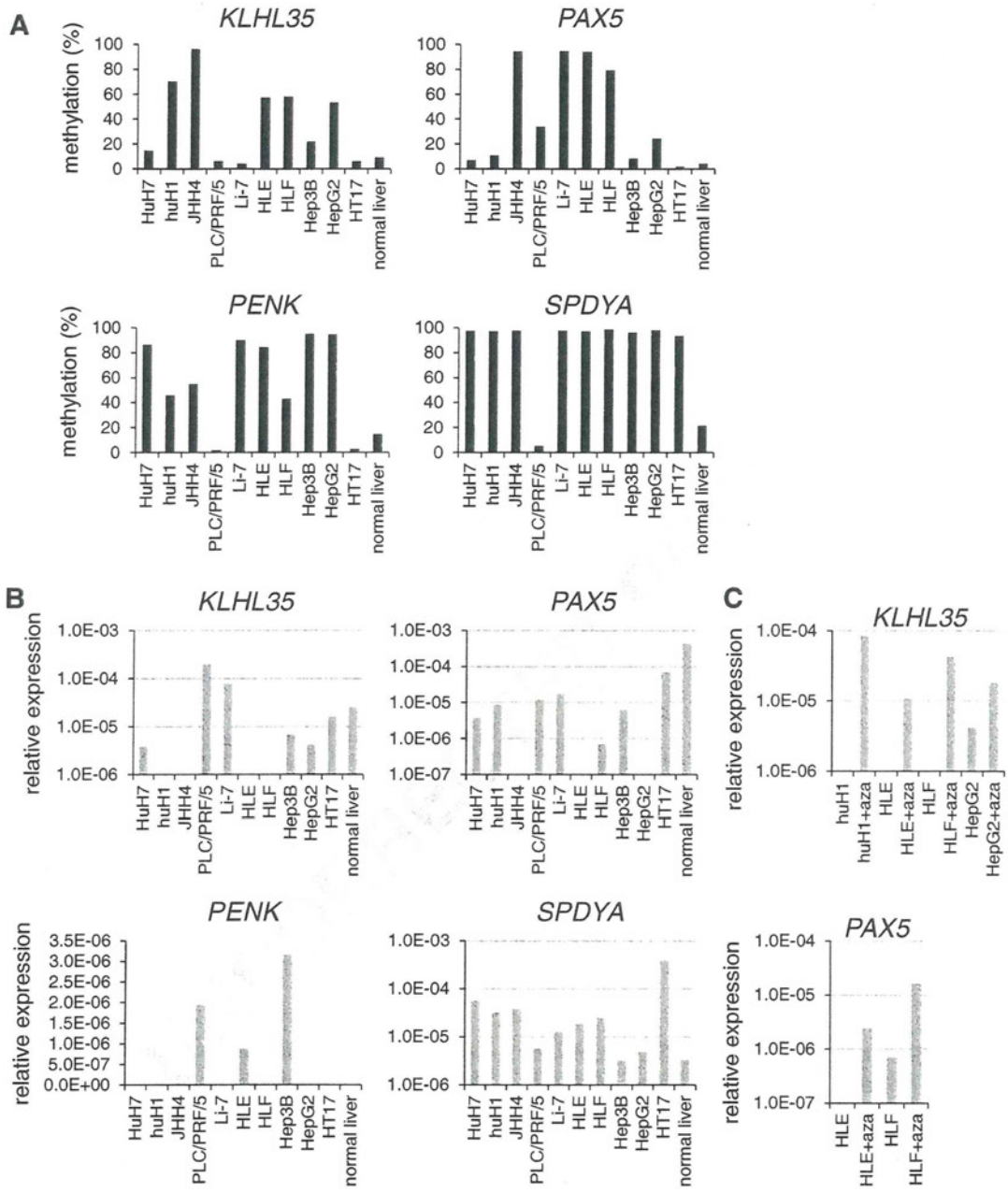

Fig. 3 Analysis of the methylation and expression of the indicated genes in HCC cell lines. **a** Bisulfite pyrosequencing of *KLHL35*, *PAX5*, *PENK*, and *SPDYA* in HCC cell lines and normal liver tissue from a healthy individual. **b** Quantitative RT-PCR of the four genes in HCC cell lines and normal liver tissue. **c** Quantitative RT-PCR of *KLHL35* and *PAX5* in HCC cell lines, with and without 5-aza-dC (*aza*) treatment

pyrosequencing, we found that levels of LINE-1 methylation were significantly lower in tumor tissues than in their noncancerous counterparts (48.5 vs. 66.8 %, $P<0.001$). LINE-1 hypomethylation was prevalent, regardless of the tumor's hepatitis virus status, but the average methylation level was lowest in the HBV/HCV-negative tumors (HBV-positive, 50.8 vs. 66.3 %, $P<0.001$; HCV-positive, 48.9 vs. 67.4 %, $P<0.001$; HBV/HCV-negative, 44.7 vs. 66.6 %, $P<0.001$; Fig. 4a). The ROC curve analysis revealed that LINE-1 methylation discriminated strongly between HCC tissue and noncancerous liver tissue (Fig. 4b), though no significant correlation was found between the levels of LINE-1 methylation and the clinicopathological characteristics of the samples (Table 1). Finally, we tested whether LINE-1 hypomethylation is linked to gene hypermethylation. We found an inverse relationship between the level of

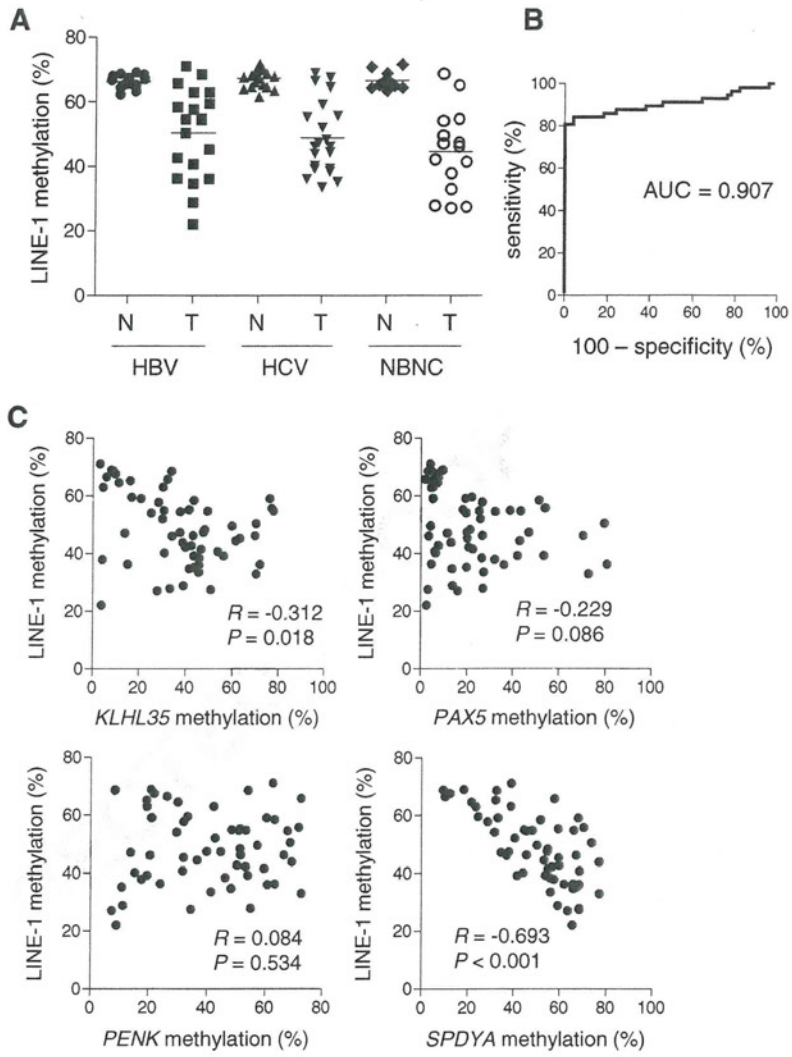

Fig. 4 Analysis of LINE-1 methylation and its association with CpG island hypermethylation in HCC. **a** Summary of bisulfite pyrosequencing analysis of LINE-1 in tumor tissue (*T*) and corresponding noncancerous liver tissue (*N*) from HBV-positive, HCV-positive, and HBV/HCB-negative (*NBNC*) HCC patients. **b** ROC curve analysis of the utility of LINE-1 methylation for distinguishing between HCC tissue and corresponding noncancerous liver tissue from the same HCC patients. **c** Correlation between the level of LINE-1 methylation and methylation of the indicated genes in HCC tissues. The Pearson correlation coefficients and *P* values are shown

LINE-1 methylation and levels of *KLHL35* and *SPDYA* methylation. On the other hand, we found no significant correlation between the LINE-1 hypomethylation and *PAX5* or *PENK* methylation (Fig. 4c).

Discussion

In the present study, we carried out high-throughput CpG island methylation profiling in a set of primary HCC tissues with and without hepatitis virus infection. MCAM analysis enabled us to evaluate the methylation status of more than 6,000 gene promoters with high specificity and sensitivity [13]. Consistent with earlier studies that showed methylation to be more abundant in the HCV-positive HCCs than in the HBV-positive or hepatitis virus-negative HCCs [15, 18], we observed the highest number of methylated genes in HCV-positive HCC tissue. However, we also noted that a large number of genes were commonly methylated among HCCs, irrespective of the hepatitis virus status, indicating that aberrant methylation of multiple genes may be involved in a common mechanism underlying hepatocarcinogenesis. Moreover, studies have also shown that aberrant methylation detected in tissues or blood samples could be a useful biomarker for early detection of HCC [19, 20]. We therefore validated the methylation status of 14 genes and identified four genes that were frequently methylated in HCC tissues but showed little or no methylation in surrounding noncancerous tissues. The high-tumor specificity suggests that methylation of these genes may not occur at precancerous stages, such as chronic hepatitis or liver cirrhosis; instead, they may be acquired during malignant transformation.

The paired box 5 (*PAX5*) gene is a member of the paired box-containing family of transcription factors, which are involved in the control of organ development and tissue differentiation [21]. PAX5 is also known to be a B cell-

specific activator protein that plays an essential role during B cell differentiation, neural development, and spermatogenesis. Methylation of the CpG island of *PAX5* was first discovered in breast cancer cells using the MCA technique [22]. Subsequently, methylation and downregulation of *PAX5* were found in lymphoid neoplasms [23]. In addition, while we are preparing the present manuscript, methylation of *PAX5* was reported in HCC and gastric cancer [24, 25]. Restoration of *PAX5* expression in HCC cells induced growth arrest and apoptosis through upregulation of various target genes, including p53, p21, and Fas ligand, suggesting that the PAX5 acts as a tumor suppressor [24].

The involvement of the kelch-like 35 (*KLHL35*) gene in cancer had not been reported until recently, when a genome-wide analysis of DNA methylation in renal cell carcinoma identified frequent hypermethylation of nine genes, including *KHLH35* [26]. Although the function of the gene product remains unknown, RNAi-induced knockdown of *KHLH35* in HEK293 cells promoted anchorage-independent growth, indicating its possible role in tumorigenesis [26].

The proenkephalin (*PENK*) gene encodes preproenkephalin, a precursor protein that is proteolytically cleaved to produce the endogenous opioid peptides met- and leu-enkephalin. Methylation of the CpG island of *PENK* was first identified in pancreatic cancer cells using the MCA technique [27]. Downregulated expression of *PENK* has also been reported in prostate cancer, suggesting its possible involvement in cancer development [28], and *PENK* methylation was recently identified in lung cancer, bladder cancer, and meningioma [29–31]. Although its functional role in cancer is not fully understood, a recent study showed that in response to cellular stress, PENK physically associates with p53 and RelA (p65) and regulates stress-induced apoptosis [32].

The *SPDYA* encodes Spy1, also known as Speedy, an atypical CDK activator known to promote cell survival, prevent apoptosis, and inhibit checkpoint activation in response to DNA damage [33]. The expression of *SPDYA* is upregulated in breast cancer [34], and its overexpression in a mouse model has been shown to accelerate mammary tumorigenesis [35]. Moreover, a recent study showed overexpression of *SYPDA* in HCC and its association with poor prognosis [36]. These results strongly suggest its involvement in oncogenesis. In the present study, we also observed that most of the HCC cell lines tested exhibited greater expression of *SPDYA* than normal liver tissue, regardless of the methylation status. Among the three transcription variants of *SPDYA* annotated in the NCBI Reference Sequence database, transcription start sites of variants 1 and 3 are located within the CpG island, while that of variant 2 are located approximately 5 kb downstream of the CpG island. Thus, the *SPDYA* transcript in HCC cells may be derived from the downstream transcription start site.

By analyzing the LINE-1 methylation levels, we and others have shown that global hypomethylation is a commonly observed feature of HCC [8, 9, 37]. Earlier studies have suggested that the association between global methylation and hepatitis status may be attributable to hepatitis B virus X protein, which can induce aberrant methylation of specific genes and global hypomethylation [38]. By contrast, we found in the present study that LINE-1 hypomethylation is prevalent among HCC tissues, regardless of the hepatitis virus infection, which suggests that global hypomethylation is involved in a common mechanism underlying hepatocarcinogenesis. It has been shown that the timing of global hypomethylation differs among tumor types. For example, hypomethylation is often observed during the early stages of colorectal and gastric carcinogenesis. By contrast, LINE-1 hypomethylation appears to be tumor-specific in HCC; it is rarely found in precancerous lesions such as chronic hepatitis or liver cirrhosis [8, 9]. A recent study showed that global hypomethylation is associated with a poorer prognosis in HCC patients [39]. In addition, the levels of serum LINE-1 hypomethylation in HCC patients reportedly correlate with serum HBs antigen status, large tumor size, and advanced tumor stage [40]. This suggests that hypomethylation may not occur at precancerous stages, and that LINE-1 methylation could be a useful biomarker with which to identify HCC and predict its clinical outcome.

The relationship between LINE-1 hypomethylation and CpG island hypermethylation in cancer is controversial. In one study, LINE-1 methylation levels were reduced in HCCs with the CpG island methylator phenotype, indicating a positive correlation between global hypomethylation and CpG island hypermethylation [9]. Another study showed that LINE-1 hypomethylation was positively correlated with hypermethylation of only a few genes (*p16*, *CACNA1G*, and *CDKN1C*), while methylation of a large number of genes showed inverse or no correlation with LINE-1 hypomethylation [12]. In the present study, we found that methylation of *KLHL35* and *SPYDA* correlates positively with LINE-1 hypomethylation, whereas levels of *PAX5* or *PENK* methylation are independent of LINE-1 methylation. These results suggest that the association between CpG island methylation and global hypomethylation may be site specific, and that hypomethylation of LINE-1 is a more generalized phenomenon than hypermethylation of CpG islands in HCC.

In summary, by screening targets of DNA methylation in HCC, we identified four frequently methylated genes. These genes are methylated in a cancer-specific manner and could be useful molecular markers for diagnosing HCC. In addition, we observed prevalent LINE-1 hypomethylation in HCC, irrespective of hepatitis virus infection. Identification of aberrant methylation in HCC may provide valuable information that not only contributes to our understanding of the pathogenesis

of the disease, but also to the development of new strategies for diagnosis and therapy.

Acknowledgments We thank Dr. Yutaka Kondo for technical advice on MCAM analysis and Masami Ashida for technical assistance. This study was supported in part by a Grant-in-Aid for Scientific Research (B) from the Japan Society for Promotion of Science (Y. Shinomura), a Grant-in-Aid for the Third-term Comprehensive 10-year Strategy for Cancer Control (M. Toyota and H. Suzuki), and a Grant-in-Aid for Cancer Research from the Ministry of Health, Labor, and Welfare, Japan (M. Toyota and H. Suzuki).

Conflicts of interest None

References

1. Parkin DM, Bray F, Ferlay J, Pisani P. Global cancer statistics, 2002. CA Cancer J Clin. 2005;55:74–108.
2. Chen CJ, Yu MW, Liaw YF. Epidemiological characteristics and risk factors of hepatocellular carcinoma. J Gastroenterol Hepatol. 1997;12:S294–308.
3. Montesano R, Hainaut P, Wild CP. Hepatocellular carcinoma: from gene to public health. J Natl Cancer Inst. 1997;89:1844–51.
4. Thorgeirsson SS, Grisham JW. Molecular pathogenesis of human hepatocellular carcinoma. Nat Genet. 2002;31:339–46.
5. Jones PA, Baylin SB. The fundamental role of epigenetic events in cancer. Nat Rev Genet. 2002;3:415–28.
6. Cordaux R, Batzer MA. The impact of retrotransposons on human genome evolution. Nat Rev Genet. 2009;10:691–703.
7. Yang AS, Estecio MR, Doshi K, Kondo Y, Tajara EH, Issa JP. A simple method for estimating global DNA methylation using bisulfite PCR of repetitive DNA elements. Nucleic Acids Res. 2004;32:e38.
8. Takai D, Yagi Y, Habib N, Sugimura T, Ushijima T. Hypomethylation of line1 retrotransposon in human hepatocellular carcinomas, but not in surrounding liver cirrhosis. Jpn J Clin Oncol. 2000;30:306–9.
9. Kim MJ, White-Cross JA, Shen L, Issa JP, Rashid A. Hypomethylation of long interspersed nuclear element-1 in hepatocellular carcinomas. Mod Pathol. 2009;22:442–9.
10. Kaneto H, Sasaki S, Yamamoto H, Itoh F, Toyota M, Suzuki H, Ozeki I, Iwata N, Ohmura T, Satoh T, Karino Y, Toyota J, Satoh M, Endo T, Omata M, Imai K. Detection of hypermethylation of the p16(ink4a) gene promoter in chronic hepatitis and cirrhosis associated with hepatitis B or C virus. Gut. 2001;48:372–7.
11. Takagi H, Sasaki S, Suzuki H, Toyota M, Maruyama R, Nojima M, Yamamoto H, Omata M, Tokino T, Imai K, Shinomura Y. Frequent epigenetic inactivation of sfrp genes in hepatocellular carcinoma. J Gastroenterol. 2008;43:378–89.
12. Lee HS, Kim BH, Cho NY, Yoo EJ, Choi M, Shin SH, Jang JJ, Suh KS, Kim YS, Kang GH. Prognostic implications of and relationship between CpG island hypermethylation and repetitive DNA hypomethylation in hepatocellular carcinoma. Clin Cancer Res. 2009;15:812–20.
13. Gao W, Kondo Y, Shen L, Shimizu Y, Sano T, Yamao K, Natsume A, Goto Y, Ito M, Murakami H, Osada H, Zhang J, Issa JP, Sekido Y. Variable DNA methylation patterns associated with progression of disease in hepatocellular carcinomas. Carcinogenesis. 2008;29:1901–10.
14. Arai E, Ushijima S, Gotoh M, Ojima H, Kosuge T, Hosoda F, Shibata T, Kondo T, Yokoi S, Imoto I, Inazawa J, Hirohashi S, Kanai Y. Genome-wide DNA methylation profiles in liver tissue at the precancerous stage and in hepatocellular carcinoma. Int J Cancer. 2009;125:2854–62.
15. Deng YB, Nagae G, Midorikawa Y, Yagi K, Tsutsumi S, Yamamoto S, Hasegawa K, Kokudo N, Aburatani H, Kaneda A. Identification of genes preferentially methylated in hepatitis C virus-related hepatocellular carcinoma. Cancer Sci. 2010;101:1501–10.
16. Goto Y, Shinjo K, Kondo Y, Shen L, Toyota M, Suzuki H, Gao W, An B, Fujii M, Murakami H, Osada H, Taniguchi T, Usami N, Kondo M, Hasegawa Y, Shimokata K, Matsuo K, Hida T, Fujimoto N, Kishimoto T, Issa JP, Sekido Y. Epigenetic profiles distinguish malignant pleural mesothelioma from lung adenocarcinoma. Cancer Res. 2009;69:9073–82.
17. Suzuki H, Yamamoto E, Nojima M, Kai M, Yamano HO, Yoshikawa K, Kimura T, Kudo T, Harada E, Sugai T, Takamaru H, Niinuma T, Maruyama R, Yamamoto H, Tokino T, Imai K, Toyota M, Shinomura Y. Methylation-associated silencing of microrna-34b/c in gastric cancer and its involvement in an epigenetic field defect. Carcinogenesis. 2010;31:2066–73.
18. Nishida N, Nagasaka T, Nishimura T, Ikai I, Boland CR, Goel A. Aberrant methylation of multiple tumor suppressor genes in aging liver, chronic hepatitis, and hepatocellular carcinoma. Hepatology. 2008;47:908–18.
19. Wong IH, Zhang J, Lai PB, Lau WY, Lo YM. Quantitative analysis of tumor-derived methylated p16ink4a sequences in plasma, serum, and blood cells of hepatocellular carcinoma patients. Clin Cancer Res. 2003;9:1047–52.
20. Zhang YJ, Wu HC, Shen J, Ahsan H, Tsai WY, Yang HI, Wang LY, Chen SY, Chen CJ, Santella RM. Predicting hepatocellular carcinoma by detection of aberrant promoter methylation in serum DNA. Clin Cancer Res. 2007;13:2378–84.
21. Carotta S, Holmes ML, Pridans C, Nutt SL. Pax5 maintains cellular identity by repressing gene expression throughout B cell differentiation. Cell Cycle. 2006;5:2452–6.
22. Palmisano WA, Crume KP, Grimes MJ, Winters SA, Toyota M, Esteller M, Joste N, Baylin SB, Belinsky SA. Aberrant promoter methylation of the transcription factor genes pax5 alpha and beta in human cancers. Cancer Res. 2003;63:4620–5.
23. Lazzi S, Bellan C, Onnis A, De Falco G, Sayed S, Kostopoulos I, Onorati M, D'Amuri A, Santopietro R, Vindigni C, Fabbri A, Righi S, Pileri S, Tosi P, Leoncini L. Rare lymphoid neoplasms coexpressing B- and T-cell antigens. The role of pax-5 gene methylation in their pathogenesis. Hum Pathol. 2009;40:1252–61.
24. Liu W, Li X, Chu ES, Go MY, Xu L, Zhao G, Li L, Dai N, Si J, Tao Q, Sung JJ, Yu J. Paired box gene 5 is a novel tumor suppressor in hepatocellular carcinoma through interaction with p53 signaling pathway. Hepatology. 2011;53:843–53.
25. Li X, Cheung KF, Ma X, Tian L, Zhao J, Go MY, et al. (2012) Epigenetic inactivation of paired box gene 5, a novel tumor suppressor gene, through direct upregulation of p53 is associated with prognosis in gastric cancer patients. Oncogene, in press. Q1
26. Morris MR, Ricketts CJ, Gentle D, McRonald F, Carli N, Khalili H, Brown M, Kishida T, Yao M, Banks RE, Clarke N, Latif F, Maher ER. Genome-wide methylation analysis identifies epigenetically inactivated candidate tumour suppressor genes in renal cell carcinoma. Oncogene. 2011;30:1390–401.
27. Ueki T, Toyota M, Skinner H, Walter KM, Yeo CJ, Issa JP, Hruban RH, Goggins M. Identification and characterization of differentially methylated cpg islands in pancreatic carcinoma. Cancer Res. 2001;61:8540–6.
28. Goo YA, Goodlett DR, Pascal LE, Worthington KD, Vessella RL, True LD, Liu AY. Stromal mesenchyme cell genes of the human prostate and bladder. BMC Urol. 2005;5:17.
29. Chung JH, Lee HJ, Kim BH, Cho NY, Kang GH. DNA methylation profile during multistage progression of pulmonary adenocarcinomas. Virchows Arch. 2011;459:201–11.

30. Chung W, Bondaruk J, Jelinek J, Lotan Y, Liang S, Czerniak B, Issa JP. Detection of bladder cancer using novel DNA methylation biomarkers in urine sediments. Cancer Epidemiol Biomarkers Prev. 2011;20:1483–91.
31. Kishida Y, Natsume A, Kondo Y, Takeuchi I, An B, Okamoto Y, et al. (2012) Epigenetic subclassification of meningiomas based on genome-wide DNA methylation analyses. Carcinogenesis, in press.
32. McTavish N, Copeland LA, Saville MK, Perkins ND, Spruce BA. Proenkephalin assists stress-activated apoptosis through transcriptional repression of nf-kappab- and p53-regulated gene targets. Cell Death Differ. 2007;14:1700–10.
33. Gastwirt RF, McAndrew CW, Donoghue DJ. Speedy/ringo regulation of CDKs in cell cycle, checkpoint activation and apoptosis. Cell Cycle. 2007;6:1188–93.
34. Zucchi I, Mento E, Kuznetsov VA, Scotti M, Valsecchi V, Simionati B, Vicinanza E, Valle G, Pilotti S, Reinbold R, Vezzoni P, Albertini A, Dulbecco R. Gene expression profiles of epithelial cells microscopically isolated from a breast-invasive ductal carcinoma and a nodal metastasis. Proc Natl Acad Sci U S A. 2004;101:18147–52.
35. Golipour A, Myers D, Seagroves T, Murphy D, Evan GI, Donoghue DJ, Moorehead RA, Porter LA. The spy1/ringo family represents a novel mechanism regulating mammary growth and tumorigenesis. Cancer Res. 2008;68:3591–600.
36. Ke Q, Ji J, Cheng C, Zhang Y, Lu M, Wang Y, Zhang L, Li P, Cui X, Chen L, He S, Shen A. Expression and prognostic role of spy1 as a novel cell cycle protein in hepatocellular carcinoma. Exp Mol Pathol. 2009;87:167–72.
37. Lin CH, Hsieh SY, Sheen IS, Lee WC, Chen TC, Shyu WC, Liaw YF. Genome-wide hypomethylation in hepatocellular carcinogenesis. Cancer Res. 2001;61:4238–43.
38. Park IY, Sohn BH, Yu E, Suh DJ, Chung YH, Lee JH, Surzycki SJ, Lee YI. Aberrant epigenetic modifications in hepatocarcinogenesis induced by hepatitis B virus X protein. Gastroenterology. 2007;132:1476–94.
39. Calvisi DF, Simile MM, Ladu S, Pellegrino R, De Murtas V, Pinna F, Tomasi ML, Frau M, Virdis P, De Miglio MR, Muroni MR, Pascale RM, Feo F. Altered methionine metabolism and global DNA methylation in liver cancer: relationship with genomic instability and prognosis. Int J Cancer. 2007;121:2410–20.
40. Tangkijvanich P, Hourpai N, Rattanatanyong P, Wisedopas N, Mahachai V, Mutirangura A. Serum line-1 hypomethylation as a potential prognostic marker for hepatocellular carcinoma. Clin Chim Acta. 2007;379:127–33.

Development 139, 667-677 (2012) doi:10.1242/dev.072272

Genetic ablation of *Rest* leads to in vitro-specific derepression of neuronal genes during neurogenesis

Hitomi Aoki[1], Akira Hara[2], Takumi Era[3], Takahiro Kunisada[1] and Yasuhiro Yamada[4,5,*]

SUMMARY

Rest (RE1-silencing transcription factor, also called Nrsf) is involved in the maintenance of the undifferentiated state of neuronal stem/progenitor cells in vitro by preventing precocious expression of neuronal genes. However, the function of *Rest* during neurogenesis in vivo remains to be elucidated because of the early embryonic lethal phenotype of conventional *Rest* knockout mice. In the present study, we have generated *Rest* conditional knockout mice, which allow the effect of genetic ablation of *Rest* during embryonic neurogenesis to be examined in vivo. We show that *Rest* plays a role in suppressing the expression of neuronal genes in cultured neuronal cells in vitro, as well as in non-neuronal cells outside of the central nervous system, but that it is dispensable for embryonic neurogenesis in vivo. Our findings highlight the significance of extrinsic signals for the proper intrinsic regulation of neuronal gene expression levels in the specification of cell fate during embryonic neurogenesis in vivo.

KEY WORDS: Rest (Nrsf), Mouse model, Neurogenesis

INTRODUCTION

The establishment and maintenance of neuronal identity underlie the core of neuronal development. The transcriptional repressor RE1-silencing transcription factor [Rest; also known as neuron-restrictive silencer factor (Nrsf)], was initially discovered as a negative regulator of neuron-specific genes in non-neuronal cells (Chong et al., 1995; Schoenherr and Anderson, 1995). Rest is expressed throughout early development, where it represses the expression of neuronal genes and is involved in the transcriptional silencing of neuronal promoters in conjunction with CoRest (Rcor1/2) (Ballas et al., 2001), which recruits additional silencing machinery, including the methyl DNA-binding protein MeCP2, histone deacetylase (HDAC) and the histone H3K9 methyltransferase G9a (Ehmt2) (Andres et al., 1999; Lunyak et al., 2002; Roopra et al., 2004; Shi et al., 2003; You et al., 2001). Rest targets include a number of genes encoding ion channels, neurotrophins, synaptic vesicle proteins and neurotransmitter receptors (Bruce et al., 2004; Johnson et al., 2006; Otto et al., 2007). Indeed, a targeted mutation of *Rest* in mice caused derepression of neuron-specific tubulin in a subset of non-neuronal tissues, leading to embryonic lethality (Chen et al., 1998).

Mosaic inhibition of *Rest* in chicken embryos using a dominant-negative form of *Rest* also caused derepression of neuronal tubulin, as well as several other neuronal target genes, not only in non-neuronal tissues but also neuronal progenitors (Chen et al., 1998). These results suggest that *Rest* is required to repress the expression of neuronal genes in undifferentiated neuronal tissue. Expression of Rest is highest in embryonic stem cells (ESCs) and is downregulated as ESCs differentiate into neuronal stem cells (NSCs), and it is completely silenced in mature adult neuronal cells (Ballas et al., 2005). Given the fact that Rest represses the expression of a large number of neuronal genes, it is reasonable to expect that it plays a central role in the inhibition of the precocious expression of neuronal genes in NSCs, and that its downregulation upon receipt of neuronal differentiation cues permits the robust expression of differentiation-related neuronal genes, resulting in terminal differentiation (Ballas et al., 2005).

In addition to the involvement of Rest in neurogenesis, recent studies have demonstrated that Rest modulates glial lineage elaboration (Abrajano et al., 2009; Kohyama et al., 2010), suggesting that it also mediates the coupling of neurogenesis and gliogenesis, which might contribute to the neuronal-glial interactions that are associated with synaptic and neuronal network plasticity and homeostasis in the brain. Despite the expectation of a fundamental role of Rest in brain development, the function of Rest in NSCs and neuronal progenitors in the brain in vivo remains to be elucidated. *Rest* null mice survive to embryonic day (E) 9 without obvious morphological defects, by which time all three germ layers and the neural tube have formed, clearly demonstrating that neuronal progenitors can develop in vivo in the absence of *Rest* (Chen et al., 1998). However, *Rest* null mice die by E11.5 accompanied by gross morphological changes starting ~E9.5. This early embryonic lethality has precluded further analysis of the role of *Rest* in the maintenance and differentiation of NSCs and neural progenitor cells (NPCs) in vivo.

In addition to the possible role of *Rest* in neuronal/glial development, recent studies have indicated that the breakdown of these processes accompanies and promotes neurodegenerative disorders. The disruption of the interaction of Rest with its target genes was reported in epileptic seizures (Bassuk et al., 2008), Huntington's disease (Zuccato et al., 2007) and Down's syndrome (Canzonetta et al., 2008; Lepagnol-Bestel et al., 2009). In these disorders, Rest dysfunction is suggested to be a cause of aberrant changes in neuronal gene expression. Considering that abnormal expression of Rest has been seen in a variety of neurological and neurodegenerative diseases, it is important to uncover the

[1]Department of Tissue and Organ Development and [2]Department of Tumor Pathology, Regeneration, and Advanced Medical Science, Gifu University Graduate School of Medicine, Gifu, 501-1194, Japan. [3]Division of Molecular Neurobiology, Institute of Molecular Embryology and Genetics, Kumamoto University, Kumamoto 860-0811, Japan. [4]PRESTO, Japan Science and Technology Agency, 4-1-8 Honcho Kawaguchi, Saitama, Japan. [5]Center for iPS Cell Research and Application (CiRA), Institute for Integrated Cell-Material Sciences (iCeMS), Kyoto University, Kyoto 606-8507, Japan.

*Author for correspondence (y-yamada@cira.kyoto-u.ac.jp)

Accepted 18 December 2011

mechanisms that underlie how Rest suppresses the expression of neuronal genes to control neurogenesis and gliogenesis, and to provide a better understanding of the pathogenesis of such diseases.

In the present study, we have generated *Rest* conditional knockout mice that allow the effects of genetic ablation of *Rest* on brain development to be examined in vivo. We also examined the effect of *Rest* ablation in cells outside of the nervous system at different developmental stages.

MATERIALS AND METHODS

Animals

All animal experiments were approved by the Animal Research Committee of the Gifu University Graduate School of Medicine. $Rest^{2lox/2lox}$ mice were generated from the $Rest^{2lox/+}$ ESC line as described preciously (Yamada et al., 2010). *Rosa26::rtTA*; *Col1a1::tetO-Cre* mice (Yamada et al., 2010) and *Sox1-Cre/+* mice (Takashima et al., 2007) were bred with $Rest^{2lox/2lox}$ mice to generate compound transgenic mice. In order to induce Cre recombinase, doxycycline (2 mg/ml) was administered in the drinking water of the mice, supplemented with 10 mg/ml sucrose (Hochedlinger et al., 2005). To induce Cre-*loxP* recombination in the embryos, pregnant female mice were treated with doxycycline in their drinking water for 5 days, and were sacrificed on the last day of the doxycycline administration. In order to label neuronal stem/progenitor cells in the adult brain, BrdU was administered as a daily intraperitoneal injection of 50 mg/kg body weight for 12 days starting at the age of 8 weeks. The brains were fixed 1 day after the last injection (Shi et al., 2004).

Cell culture

For the neurosphere culture, brains were collected and dissociated into single-cell suspensions by gentle pipetting. The inner part of the trunk region was collected for genotyping. The primary neurospheres were formed from 1×10^5 suspended brain cells/well in a 24-well plate. The cells were cultured in DMEM/F12 supplemented with 1× N2 (Invitrogen), 1× B27 (Invitrogen), 20 ng/ml epidermal growth factor (EGF) (R&D Systems) and 20 ng/ml basic fibroblast growth factor (bFGF, or FGF2) (R&D Systems). The primary neurospheres were passaged to generate secondary neurospheres, which were used to compare neurosphere formation ability. For the adherent cultures of neurospheres, the spheres were inoculated into 6-well plates previously coated with fibronectin/laminin (both from Invitrogen) and cultured in DMEM/F12 supplemented with 1× B27 and 10% fetal calf serum (FCS) (Nichirei Bioscience, Tokyo, Japan).

MEFs were derived from small pieces of the outer part of the trunk region prepared as described above. The cells were seeded in 100-mm dishes and cultured in DMEM supplemented with 10% FCS. In order to induce *Rest* recombination in vitro, cultured cells were treated with doxycycline at 2 μg/ml. The cells were analyzed for GFP signals using a FACS Aria dual-laser flow cytometer (Becton-Dickinson).

Histology and immunohistochemistry

The brains were enucleated and fixed by immersion overnight in 10% formalin in phosphate buffer (pH 7.2). Specimens were dehydrated with ethanol, soaked in xylene and embedded in paraffin. Horizontal serial sections were prepared at 3μm using a Leica RM2125RT microtome and stained with Hematoxylin and Eosin (HE).

For immunohistochemistry, we used a Mouse-to-Mouse HRP Ready-To-Use Kit (ScyTek Laboratories) according to the manufacturer's protocol to detect the mouse monoclonal primary antibodies on the sections. For detection of the goat or rabbit polyclonal primary antibodies, a Histofine Kit (Nichirei Bioscience, Tokyo, Japan) or VECTASTAIN ABC Kit (Vector Laboratories) was used according to the manufacturers' protocol. Finally, the sections were stained with 3,3′-diaminobenzidine (DAB). For immunocytochemistry studies, cells were fixed with 4% PFA, made permeable by immersion in 0.1% Triton X-100, washed in PBS and blocked in 0.5% BSA. Primary antibodies were then added and allowed to react for 60 minutes at room temperature. After washing in PBS, the cells were stained with secondary antibodies. Cells were examined using an Olympus IX-71 fluorescence microscope.

Antibodies

The primary antibodies used in this study were: anti-mouse neuronal class III beta-tubulin (Tuj1; 1:5000; BabCO); anti-mouse glial fibrillary acidic protein (Gfap; 1:1000; Dako-Cytomation, Glostrup, Denmark); anti-human nestin (1:500; IBL, Gunma, Japan); anti-mouse nestin (1:1000; Chemicon); anti-mouse NeuN (1:1000; Chemicon); anti-BrdU (1:500; Dako-Cytomation); anti-doublecortin (Dcx; 1:500; Santa Cruz); anti-Prox1 (1:5000; Millipore); anti-radial glial cell marker 2 (clone RC2; 1:300; Millipore); anti-trimethyl histone H3 (Lys27) (1:200; Monoclonal Institute, Hokkaido, Japan).

Gene expression analysis

Total RNA was prepared using the RNeasy Plus Mini Kit (Qiagen) according to the manufacturer's instructions. The first-strand cDNA was synthesized from 1 μg total RNA using the SuperScript First-Strand Synthesis System (Takara, Shiga, Japan) with oligo(dT) primers. Real-time PCR was performed with SYBR Premix EX Taq (Takara) using Thermal Cycler Dice (Takara) for each gene of interest, and a β-actin endogenous control primer set was used for normalization. The primer sequences used in qRT-PCR analyses were obtained from PrimerBank (http://pga.mgh.harvard.edu/primerbank/).

The microarray analysis was performed according to the manufacturer's instructions (materials from Agilent unless otherwise stated). Briefly, cyanine-3 (Cy3)-labeled cRNA was prepared from 100 ng RNA using the One-Color Low RNA Input Liner Amplification Kit, followed by RNeasy column purification (Qiagen). Dye incorporation and cRNA yield were checked with a NanoDrop ND-1000 spectrophotometer. A total of 1.5 μg of Cy3-labeled cRNA (specific activity >10.0 pmol Cy3/μg cRNA) was fragmented at 60°C for 30 minutes in a reaction volume of 50 μl containing 1× fragmentation buffer and 2× blocking agent following the manufacturer's instructions. On completion of the fragmentation reaction, 50 μl 2× HI-RPM Hybridization Buffer was added and hybridized to Whole Mouse Genome Oligo Microarrays (G4122F) for 17 hours at 65°C in a rotating hybridization oven. After hybridization, microarrays were washed for 1 minute at room temperature with GE Wash Buffer 1 and 1 minute at 37°C with GE Wash buffer 2, then dried immediately by brief centrifugation. Slides were scanned immediately after washing on a DNA microarray scanner (G2565B) using the one-color scan setting for 4×44k array slides [scan area 75×25 mm, scan resolution 5 μm, dye channel set to green and green PMT set to 10-100% (XDR)]. The scanned images were analyzed with the Feature Extraction Software package v. 9.5.3.1 using default parameters (protocol GE1-v5_95_Feb07 and Grid: 014868_D_F_20101102) to obtain background-subtracted and spatially detrended processed signal intensities. Data were analyzed using GeneSpring software.

RESULTS

Conditional ablation of the CoRest binding site in developing embryos results in embryonic lethality

In order to examine the effect of *Rest* deletion in vivo, we generated mice containing floxed *Rest* alleles and doxycycline-inducible *Cre* alleles ($Rest^{2lox/2lox}$; *Rosa26::rtTA*; *Col1a1::tetO-Cre*), in which exon 4, which encodes the CoRest binding site, can be removed upon treatment of mice with doxycycline (Fig. 1A) (Andres et al., 1999; Beard et al., 2006; Fink et al., 1999; Hatano et al., 2011; Yamada et al., 2010). Rest contains two repressor domains (Tapia-Ramirez et al., 1997): an N-terminal domain that associates with HDACs and Sin3; and a C-terminal domain that interacts with CoRest (Andres et al., 1999). Importantly, although our recombined *Rest* knockout (KO) allele ($Rest^{1lox}$) still contains exons 1-3, which encode the N-terminal domain of Rest, altered *Rest* transcript was not detected in our $Rest^{1lox/1lox}$ mouse ESCs, suggesting that the $Rest^{1lox}$ allele in this system is equivalent to the conventional KO allele (Yamada et al., 2010). We further demonstrated that *Stmn2* (*SCG10*), a CoRest-independent target of Rest-mediated repression (Jepsen et al., 2000; Lunyak et al., 2002),

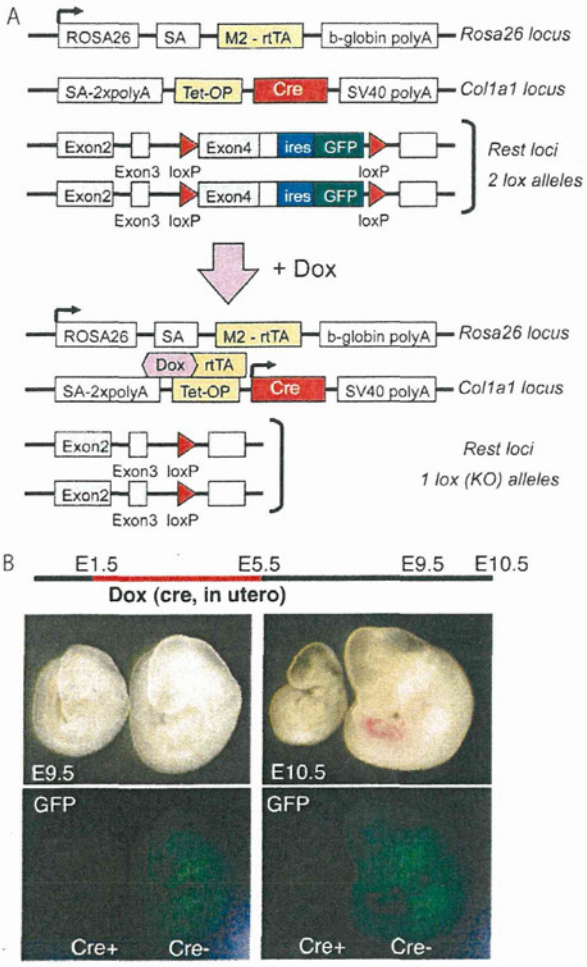

Fig. 1. Conditional *Rest* knockout mice. (**A**) In the conditional *Rest* knockout (KO) mice, exon 4 of *Rest* can be removed by doxycycline (Dox) exposure. (**B**) Pregnant mice with *Rest* conditional KO embryos were treated with doxycycline to delete the *Rest* alleles from the embryos in utero (E1.5-5.5). The growth retardation phenotype is detectable at E9.5 and E10.5.

is upregulated in $Rest^{1lox/1lox}$ mouse ESCs (supplementary material Fig. S1), indicating again that our *Rest* KO cells are equivalent to the *Rest* null cells.

A previous study using conventional KO mice revealed that mice lacking the *Rest* gene die during early embryonic development (Chen et al., 1998). When we administrated doxycycline to the *Rest* conditional KO embryos to delete the *Rest* gene in utero (E1.5-5.5), we observed lethality of the embryos carrying the *tetO-Cre* allele at ~E10.5 with a growth retardation phenotype, which was accompanied by the loss of GFP signals, indicating that the phenotype of the conventional KO mice could be recapitulated in our *Rest* conditional KO mice (Fig. 1B).

Genetic ablation of *Rest* in non-neuronal cells outside of the central nervous system in vitro

Previous studies suggest that *Rest* is expressed in a variety of non-neuronal cells to suppress the neuronal differentiation of these cells. Indeed, the conventional *Rest* KO mice showed ectopic expression of Rest target genes, such as *Tuj1* (*Tubb3*), in non-neuronal cells outside of the brain (Chen et al., 1998). Therefore, to elucidate whether *Rest* ablation can induce the expression of Rest target genes in non-neuronal cells, we used mouse embryonic fibroblasts (MEFs) containing floxed *Rest* alleles and doxycycline-inducible *Cre* alleles ($Rest^{2lox/2lox}$; *Rosa26*::*rtTA*; *Col1a1*::*tetO-Cre*). The *Rest* conditional KO MEFs were treated with doxycycline for 3 days starting 1 day after the seeding of the MEFs (passage 1). Seven days after the seeding of the MEFs, the MEFs were examined for GFP expression by FACS analysis. Three weeks after the seeding of the MEFs, they were analyzed by immunocytochemistry with a Tuj1 antibody to detect expression of the neural cell marker. The expression of Rest target genes was also examined by real-time RT-PCR 3 weeks after the seeding of the MEFs.

Consistent with the recombination, FACS analysis revealed a decreased GFP signal in the *Rest* conditional KO MEFs treated with doxycycline (Fig. 2A). As demonstrated in a previous study using conventional KO mice, deletion of *Rest* caused an increase in the expression of Tuj1 in MEFs (Fig. 2B) (Chen et al., 1998). The real-time RT-PCR revealed that MEFs treated with doxycycline expressed a significantly reduced level of *GFP* and *Rest* (Fig. 2C). We found that this was associated with increased expression of *Syt4*, *Tubb3* and *Calb1*, which contain RE1 sites and are targets of the Rest repressor complex (Chong et al., 1995; Johnson et al., 2008; Schoenherr and Anderson, 1995; Schoenherr et al., 1996) (Fig. 2C). We also found that *Stmn2*, a CoRest-independent target of Rest-mediated repression, was also derepressed in MEFs by doxycycline exposure (Fig. 2C). These results indicate that Rest target genes are rapidly derepressed upon the loss of *Rest* in MEFs. However, *Bdnf*, which also contains an RE1 site and is a target of the Rest repressor complex in ESCs/NSCs (Johnson et al., 2008; Yamada et al., 2010), did not show any detectable derepression in doxycycline-treated MEFs (Fig. 2C).

Although we confirmed that removal of the *Rest* CoRest binding site induces ectopic neuronal gene expression in non-neuronal cells outside of the brain, it remains unclear whether *Rest* ablation can actually induce neuronal differentiation in non-neuronal cells. In the present study, despite the observed increase in the expression of neuronal genes such as *Syt4*, *Tubb3*, *Calb1* and *Stmn2* after ablation of *Rest* in MEFs, the morphology of the Tuj1-expressing cells did not change (Fig. 2B). In addition, the expression of *Fsp1* (*S100a4*), a marker for fibroblasts (Strutz et al., 1995), was not decreased in the Tuj1-expressing MEFs (supplementary material Fig. S2). These findings suggest that *Rest* ablation in non-neuronal cells leads to ectopic neuronal gene expression, but that its ablation is not sufficient to induce transdifferentiation into neuronal cells (Vierbuchen et al., 2010).

We also examined the effect of *Rest* ablation in adult non-neuronal cells in vitro using tail tip fibroblasts (TTFs) containing the floxed *Rest* alleles and doxycycline-inducible *Cre* alleles. After exposure to doxycycline, we detected significant upregulation of the Rest target genes *Syt4*, *Tubb3*, *Calb1* and *Stmn2* in the TTFs, which was accompanied by the downregulation of *Rest* and *GFP* expression (supplementary material Fig. S3). Consistent with the results in MEFs, we failed to detect derepression of *Bdnf* or downregulation of *Fsp1* in TTFs after *Rest* ablation (supplementary material Fig. S3). We also conditionally deleted the *Rest* CoRest binding site in adult mice by the administration of doxycycline in the drinking water, and examined the expression of Rest target genes in the tail tissues. We confirmed the derepression of Rest target genes in the adult tail tissues after genetic ablation of *Rest* in vivo (supplementary material Fig. S4).

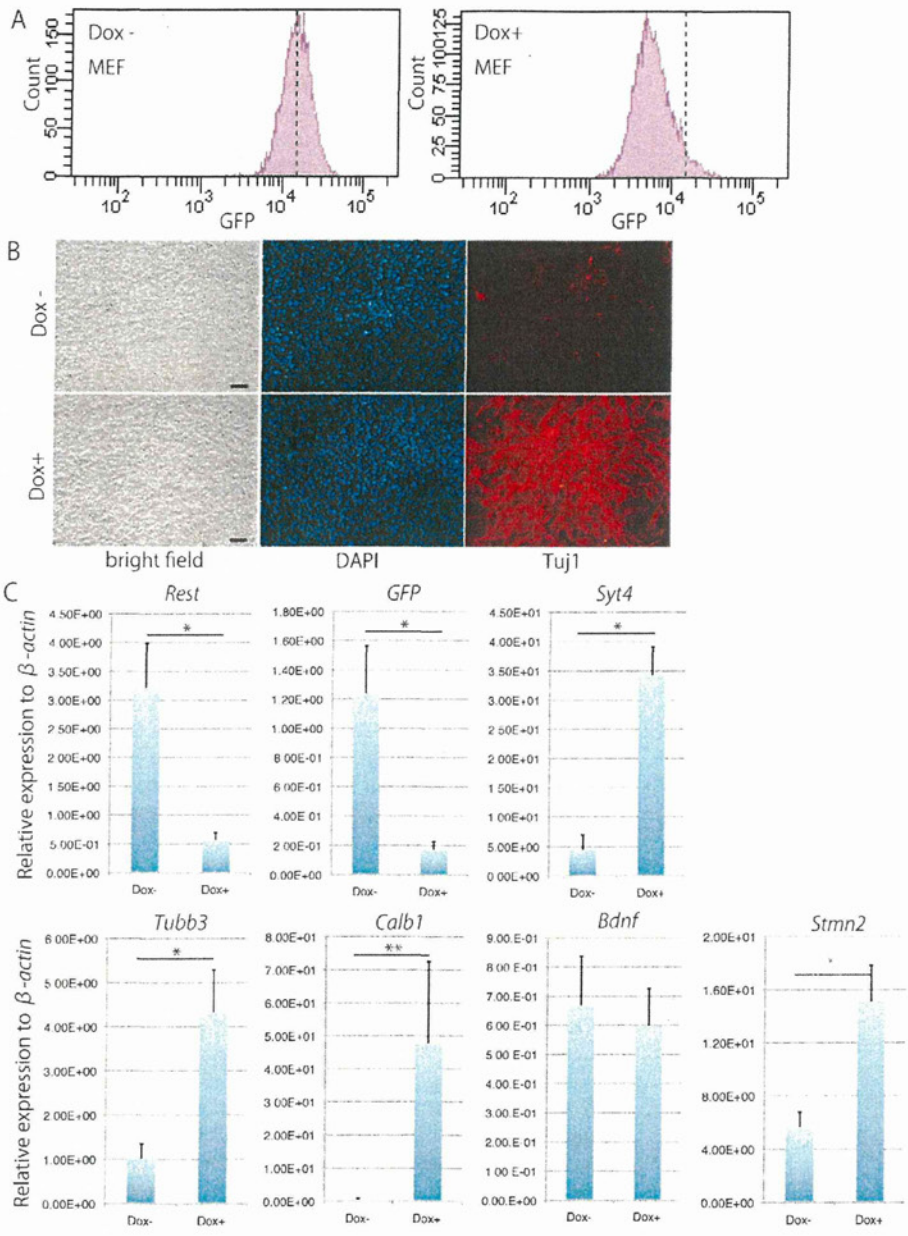

Fig. 2. The conditional deletion of *Rest* in mouse embryonic fibroblasts leads to derepression of Rest target genes. (**A**) FACS analysis revealed a decreased signal for GFP fluorescence in doxycycline-treated mouse embryonic fibroblasts (MEFs) 7 days after seeding of the MEFs. The dashed line indicates the GFP signal at the peak of the histogram of the control cells for comparison. (**B**) The conditional deletion of *Rest* in MEFs resulted in an increased number of Tuj1-positive cells in vitro. Tuj1 expression was also observed in some postmitotic neuronal cells with long axons, which were likely to be contaminating neuronal cells present in the MEF culture. Scale bars: 100 μm. (**C**) Transcript levels of *Rest*, *GFP* and Rest target genes. The expression levels of the Rest target genes *Syt4*, *Tubb3*, *Calb1* and *Stmn2* were significantly upregulated, whereas the expression levels of *Rest* and *GFP* were downregulated after *Rest* ablation in MEFs. No significant change was detectable in the *Bdnf* expression level. Transcript levels were normalized to β-actin levels. The data are presented as average values with s.d. of nine independent samples. *, $P<0.00001$; **, $P<0.0005$.

In vitro ablation of *Rest* in neuronal progenitor cells

Rest is downregulated in the brain as gestation progresses (Ballas et al., 2005). We first examined the expression of *Rest* in the developing mouse brain. The conditional KO alleles contain IRES-*GFP* sequences at the 3′ UTR of the *Rest* gene, which enable us to detect the expression and distribution of *Rest* by the GFP signals. By analyzing GFP expression, we confirmed that cells in the brain at E13.5 actually express the *Rest* gene (Fig. 3A).

In order to investigate the effect of genetic ablation of *Rest* during neurogenesis in vitro, we generated neurospheres from the brains of E13.5 *Rest* conditional KO embryos carrying the doxycycline-inducible *Cre* alleles. The primary neurospheres were passaged to form secondary neurospheres. Doxycycline was administered for 3 days starting 1 day after the passage of the primary neurospheres (passage 1). When we measured the number of secondary neurospheres in order to compare the formation of neurospheres in the presence and absence of doxycycline, the number of neurosphere cells was not significantly different 1 week after passage, regardless of doxycycline exposure (Fig. 3B). By contrast, the number of cells constituting the neurospheres exposed to doxycycline was significantly decreased after long-term culture of the neurospheres (Fig. 3C), suggesting that the ablation of *Rest* inhibited the growth of the neurospheres. Since a recent study demonstrated that *Rest* ablation in cultured neurosphere cells actually results in decreased proliferation (Gao et al., 2011), the decreased proliferative activity might be responsible for the decreased number of cultured cells upon doxycycline treatment in vitro.

We next cultured *Rest* conditional KO neurospheres (*Rest*$^{2lox/2lox}$; *Rosa26::rtTA*; *Col1a1::tetO-Cre*) under differentiation conditions. To examine the effects of *Rest* ablation on neuronal differentiation, the

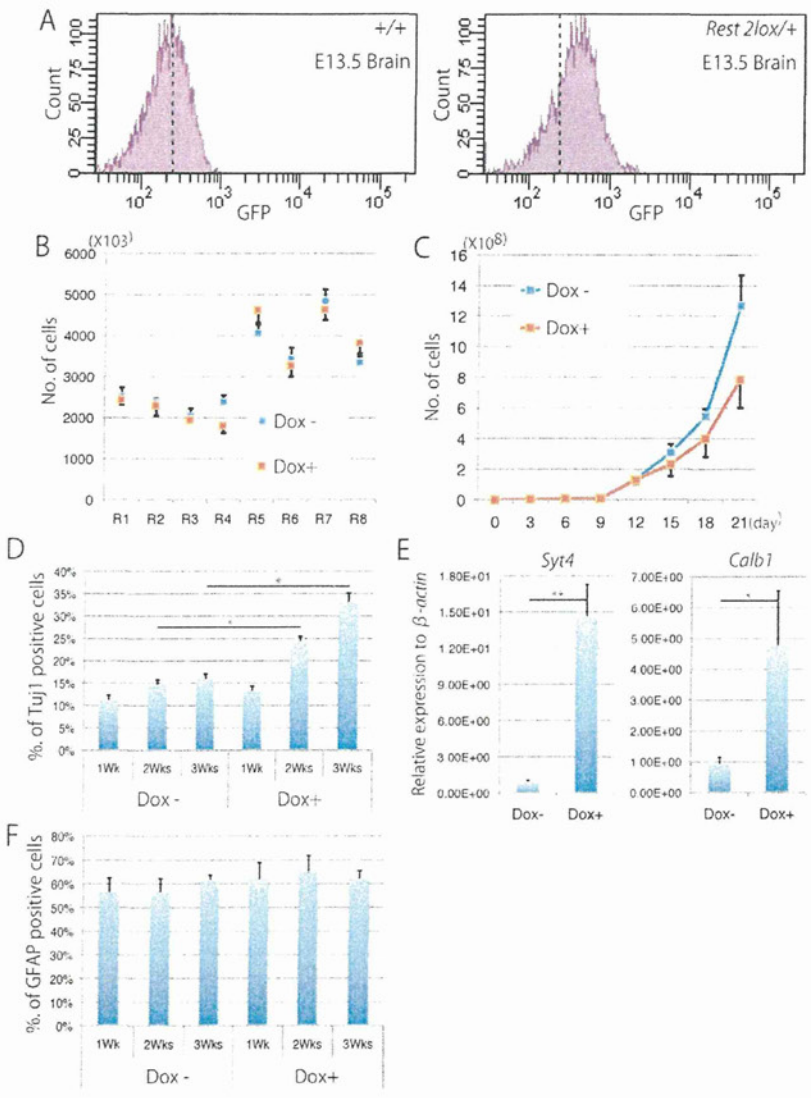

Fig. 3. *Rest* ablation in in vitro cultured neuronal cells. (**A**) FACS analysis for GFP fluorescence. The Rest^{2lox} allele contains IRES-GFP sequences at the 3′UTR of the *Rest* gene, which allows visualization of *Rest* expression via GFP signals. Cells in the E13.5 mouse brain expressed GFP, suggesting that *Rest* is expressed in the developing brain. Dashed line represents the GFP signal at the peak of the histogram of the control cells for comparison. (**B**) The number of neurosphere cells in the presence and absence of doxycycline. The data are presented as the mean number of neurosphere cells in eight independent experiments (R1-R8). Error bars indicate s.d. (**C**) The number of cells constituting neurospheres in the presence and absence of doxycycline. Doxycycline-treated neurospheres grew more slowly than control neurospheres. Error bars indicate s.d. (**D**) The percentage of Tuj1-positive cells among total differentiated neurosphere cells after genetic deletion of *Rest*. The number of Tuj1-positive cells among total cells was significantly increased after *Rest* ablation. The data are presented as average values with s.d. of three independent samples. (**E**) The expression of *Syt4* and *Calb1* is derepressed after *Rest* ablation in neurosphere-derived differentiated cells. Transcript levels were normalized to β-actin levels. The data are presented as average values with s.d. of six independent samples. (**F**) The percentage of Gfap-positive cells among total differentiated neurosphere cells after genetic deletion of *Rest*. The number of Gfap-positive cells among total cells did not change following genetic ablation of *Rest*. The data are presented as average values with s.d. of three independent samples. *, $P<0.001$; **, $P<0.00005$.

doxycycline treatment was started 1 day after seeding the neurospheres in adherent culture, and the cells were treated with doxycycline for an additional 3 days. The adherent spheres were stained with anti-Tuj1 and anti-Gfap antibodies 1, 2 and 3 weeks after doxycycline exposure (Fig. 3D and supplementary material Fig. S5) and we counted the number of Tuj1-positive or Gfap-positive cells and DAPI-positive (total) nuclei in three independent areas of 1.5 mm^2 to calculate the proportion of Tuj1-positive or Gfap-positive cells. The doxycycline-treated cells contained a significantly increased percentage of Tuj1-positive cells among total cells than the control non-treated cells after 2 and 3 weeks of the treatment (Fig. 3D). In addition, a real-time PCR analysis revealed that the expression levels of *Syt4* and *Calb1* increased in the neurosphere adherent culture after genetic ablation of *Rest* (Fig. 3E). By contrast, the percentage of Gfap-positive glial cells among total cells was not altered (Fig. 3F), suggesting that ablation of *Rest* does not have a significant effect on glial differentiation in vitro in this experimental condition.

Because the Tuj1 and Gfap double-negative cells in the adherent spheres decreased after doxycycline treatment, *Rest* ablation may induce Tuj1 expression in such Tuj1 and Gfap double-negative cells. Immunocytochemical analysis of doxycycline-treated neurosphere cells revealed that a subset of non-neuron-like cells expresses Tuj1 and/or calbindin, whereas non-neuron-like cells in the control neurospheres did not express these markers (supplementary material Fig. S6A,B). Consistent with a previous study (Gao et al., 2011), we observed a small number of cells that express both Tuj1 and Gfap, suggesting the misexpression of Rest target genes (supplementary material Fig. S6C). Collectively, these results suggest that derepression of Rest target genes occurred in the adherent neurosphere cells upon *Rest* ablation, and that this derepression might play a role in the promotion of neuronal differentiation.

The in vivo effects of *Rest* ablation on gene expressions in non-neuronal and neuronal cells of the developing embryo

In the E13.5 mouse embryo the expression level of *Rest* in the limb was higher than that in the brain (supplementary material Fig. S7). By contrast, the expression level of Rest target genes was higher in the brain than in the limb (supplementary material Fig. S7).

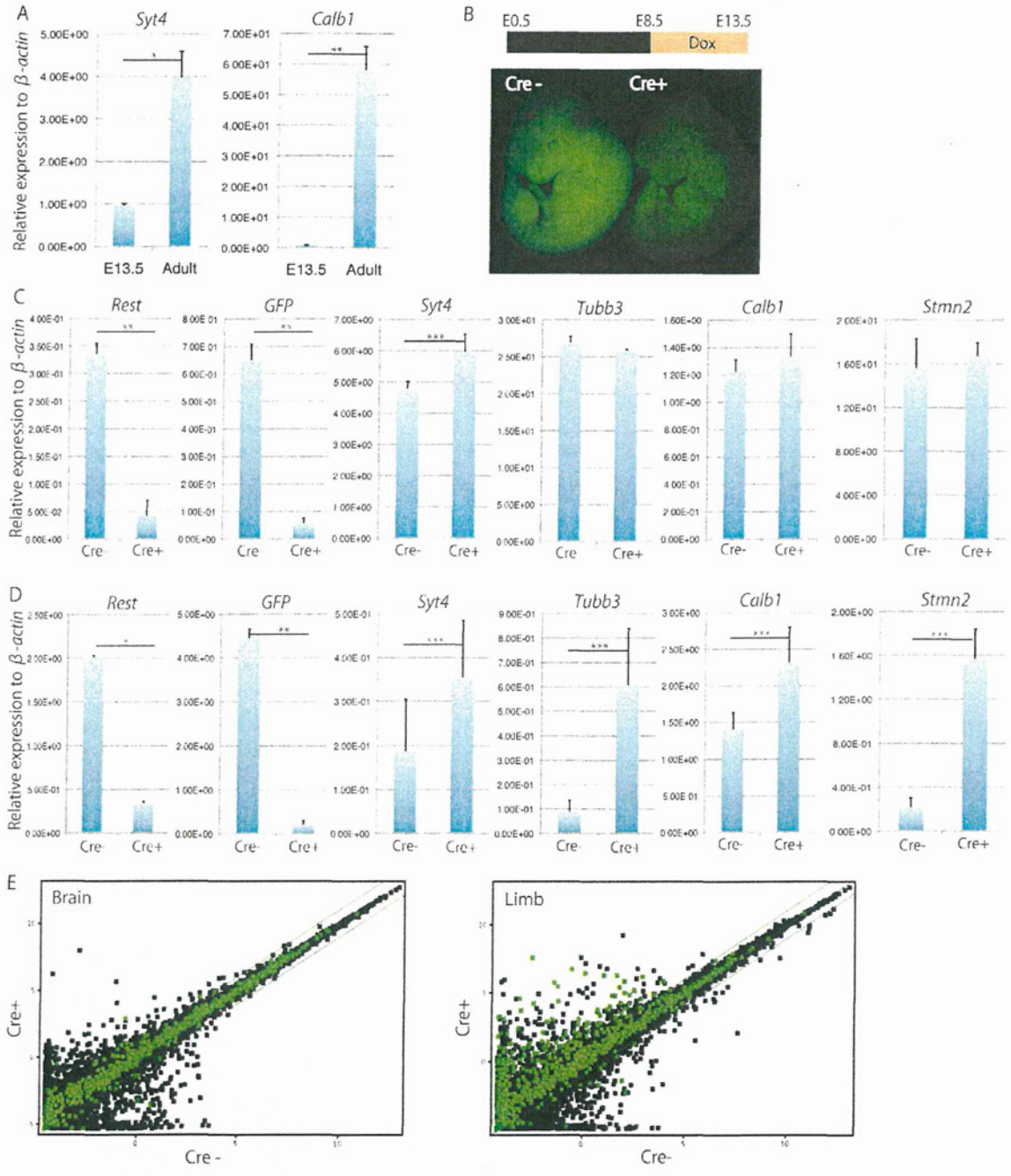

Fig. 4. In vivo genetic ablation of *Rest* in developing embryos. (**A**) Neuronal gene expression levels in the brains of E13.5 embryos and adult mice. The expression of *Syt4* and *Calb1* was significantly higher in the adult brain, suggesting that Rest neuronal target genes are still repressed in the E13.5 brain. The transcript levels were normalized to β-actin. The data are presented as average values with s.d. of six independent samples. (**B**) The experimental protocol for recombination of the *Rest* alleles in vivo. Pregnant mice with *Rest* conditional KO embryos were treated with doxycycline for 5 days, and embryos were sacrificed at E13.5. GFP fluorescence was decreased in embryos with the *tetO-Cre* allele, as compared with control embryos without the *tetO-Cre* allele. (**C**) The in vivo expression of Rest target genes in the brain. Although the expression levels of *Rest* and *GFP* were significantly downregulated, the expression levels of most Rest target genes were not derepressed in the brains of *Cre+* embryos. Transcript levels were normalized to β-actin. The data are presented as average values with s.d. of four independent samples. (**D**) The expression of Rest target genes in the peripheral tissues (limb) in vivo. The expression of *Syt4, Tubb3, Calb1* and *Stmn2* was derepressed after genetic deletion of *Rest*. Transcript levels were normalized to β-actin. The data are presented as average values with s.d. of four independent samples. (**E**) A microarray analysis of E13.5 brain and non-neuronal (limb) tissue after genetic ablation of *Rest*. Rest binding genes in neuronal stem cells (Johnson et al., 2008) are shown as green dots. Rest target genes were significantly upregulated in the *Rest*-deleted non-neuronal tissue (limb). By contrast, the derepression of Rest target genes in the brain was not observed following genetic ablation of *Rest*. *, $P<0.01$; **, $P<0.005$; ***, $P<0.05$.

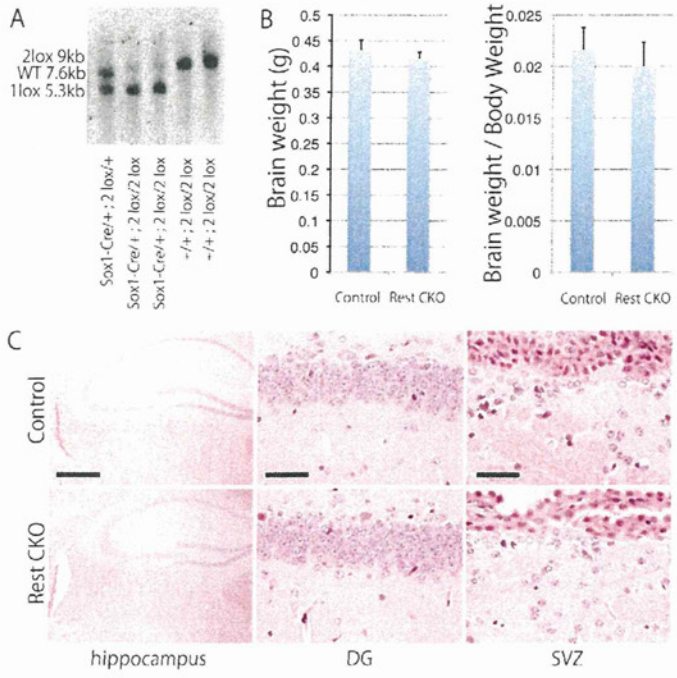

Fig. 5. The effect of *Rest* ablation on neurogenesis in vivo. (**A**) Southern blot analysis revealed that *Rest* conditional KO (2lox, 9kb) alleles in the adult brain with the *Sox1-Cre* allele recombined to form KO (1lox, 5.3kb) alleles. The wild-type (WT) allele appeared at 7.6 kb. (**B**) Comparison of brain weight and the ratio of brain weight to body weight in 8-week-old *Rest* conditional KO and control mice. Neither the brain weight nor the ratio was significantly different in *Sox1-Cre/+*; $Rest^{2lox/2lox}$ adult mice compared with control littermates. (**C**) The histology of adult brains from *Sox1-Cre/+*; $Rest^{2lox/2lox}$ mice (8 weeks of age). No histological differences were detectable in the dentate gyrus (DG, middle) of the hippocampus (left) and subventricular zone (SVZ, right) of the brains from *Sox1-Cre/+*; $Rest^{2lox/2lox}$ versus control adult mice by HE staining. Scale bars: 50 μm in DG and SVZ; 500 μm in hippocampus.

However, the expression levels of *Syt4* and *Calb1* in the E13.5 brain were significantly lower than those in the adult brain (Fig. 4A). These observations are consistent with the hypothesis that the expression of Rest target genes is still repressed in the E13.5 brain in vivo. Since our in vitro experiments revealed that the genetic ablation of *Rest* results in the increased expression of Rest target genes in both non-neuronal and neuronal cells, we next tried to dissect the effects of *Rest* ablation on the non-neuronal and neuronal cells in vivo using embryos with floxed *Rest* genes and doxycycline-inducible *Cre* alleles. The *Rest* conditional KO embryos were treated with doxycycline in utero (E8.5-13.5) to induce Cre-mediated recombination in both non-neuronal and neuronal cells, and the mice were sacrificed at E13.5 (Fig. 4B). In accordance with the recombination, E13.5 embryos with a *tetO-Cre* allele had decreased signals for GFP when compared with embryos without a *tetO-Cre* allele (Fig. 4B). We also collected the brains and limbs from *Rest*-deleted embryos and their control littermates without the *tetO-Cre* allele. Consistent with the decreased GFP signals, real-time RT-PCR analysis revealed that the expression of *Rest* was significantly downregulated in both the brain and limbs from embryos with a *tetO-Cre* allele compared with those from control littermates (Fig. 4C,D).

Similar to the results obtained in vitro, we detected a significant increase in the expression of *Syt4*, *Tubb3*, *Calb1* and *Stmn2* in the limbs of embryos with the *tetO-Cre* allele (Fig. 4D). By contrast, the expression level of *Tubb3*, *Calb1* and *Stmn2* in the brains of E13.5 embryos with a *tetO-Cre* allele remained repressed, whereas the expression levels of *Rest* and *GFP* itself were downregulated in the same samples (Fig. 4C). Although the expression of *Syt4* was slightly upregulated in the brain of embryos with a *tetO-Cre* allele (Fig. 4C), the effect was only modest when compared with the levels in the adult brain (Fig. 4A). Immunohistochemical analysis confirmed that there was no alteration in the expression pattern of Tuj1 in the E13.5 brain of embryos with a *tetO-Cre* allele (supplementary material Fig. S8A). We also examined the expression of Rest target genes in the brain or tail of E16.5 embryos with a *tetO-Cre* allele, and found no altered expression levels of these genes in brains, whereas a significant increase in the expression of *Syt4*, *Calb1* and *Stmn2* was observed in the tail (supplementary material Fig. S8B). These results indicate that the Rest target genes are specifically derepressed in non-neuronal cells outside of the brain by the genetic ablation of *Rest* in vivo.

We next performed a microarray analysis to determine the changes in gene expression after genetic deletion of *Rest* in E13.5 brain and limb in vivo. Consistent with the results of the real-time RT-PCR analysis, Rest target genes were significantly upregulated in the *Rest*-deleted limb tissue (Fig. 4E; genes interacting with Rest in ESCs and NPCs are represented by green dots) (Johnson et al., 2008). However, the derepression in the limb tissues (upregulated more than 2-fold after *Rest* ablation) was observed in only a subset of the genes with a Rest binding site (27% of the genes; Fig. 4E, limb), suggesting gene-specific derepression. By contrast, only 2% of the genes with a Rest binding site were upregulated more than 2-fold in the brain, suggesting that the derepression only occurs at a minority of Rest target genes after the genetic ablation of *Rest* (Fig. 4E, brain).

In vivo ablation of *Rest* in progenitor cells of the developing brain

Sox1 was shown to be one of the earliest transcription factors expressed in ectoderm cells committed to a neural fate (Pevny et al., 1998; Takashima et al., 2007). The expression of *Sox1* starts at E7.5-8.5 in the neural tube (Takashima et al., 2007). We used a *Sox1-Cre* allele (Takashima et al., 2007) ($Rest^{2lox/2lox}$; *Sox1-Cre/+*) to excise the floxed *Rest* genes in early progenitor cells of the developing mouse brain in vivo. The brains from *Rest* conditional KO mice carrying the *Sox1-Cre* allele ($Rest^{2lox/2lox}$; *Sox1-Cre/+*) and control littermates ($Rest2^{lox/2lox}$) were collected at E13.5, E16.5 and postnatal day (P) 0 and the expression levels of Rest target genes were compared by real-time RT-PCR. The brains from

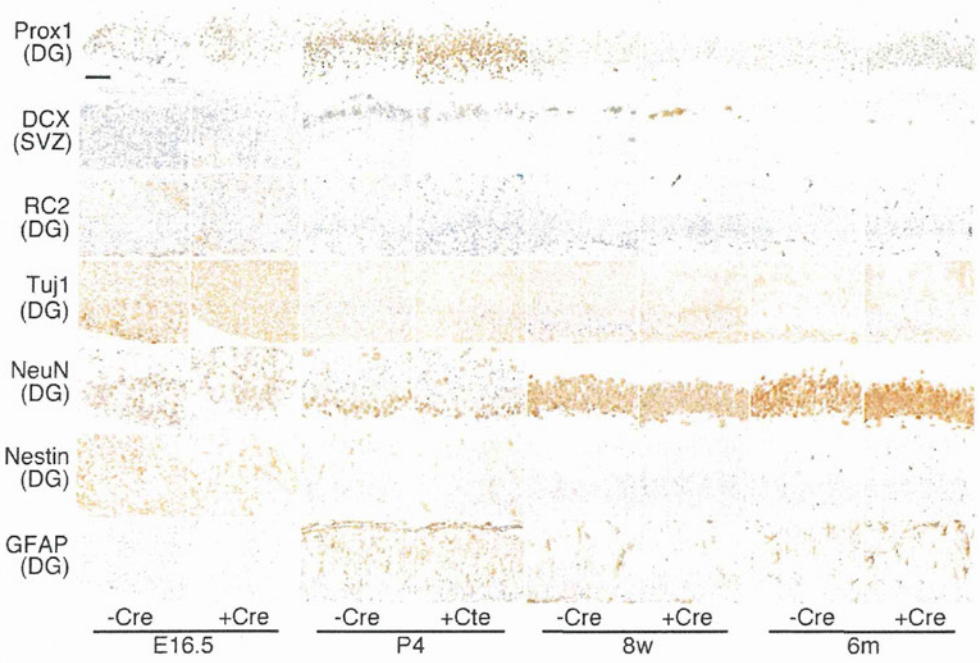

Fig. 6. Sequential immunohistochemical analysis for Prox1, Dcx, RC2, Tuj1, NeuN, nestin and Gfap. Brains at E16.5, P4, 8 weeks (8w) and 6 months (6m) of *Rest*-deficient and control mice were analyzed. DG, dentate gyrus; SVZ, subventricular zone. Scale bar: 50 μm.

embryos carrying *Sox1-Cre* had significantly lower levels of both *Rest* and *GFP* expression at all time points, reflecting the genetic ablation of *Rest* (supplementary material Fig. S9). However, consistent with the results in the experiments using doxycycline-inducible *Cre* mice, the expression levels of Rest target genes such as *Syt4*, *Tubb3*, *Calb1*, *Bdnf* and *Stmn2* (except for *Stmn2* at E13.5) were not significantly increased in the brains of developing embryos with the *Sox1-Cre* allele (supplementary material Fig. S9). These results confirm that the conditional deletion of *Rest* does not substantially affect the expression of Rest neuronal target genes in the developing brain.

Rest ablation during adult neurogenesis in vivo

To further examine the function of *Rest* in the maintenance of neurogenesis in adult brain tissue, we analyzed the brains of adult *Rest* conditional KO mice carrying the *Sox1-Cre* allele. Contrary to our expectation, the *Rest* conditional KO mice carrying the *Sox1-Cre* allele were apparently normal and grew into adults. These mice were viable for more than 1.5 years and were fertile. A Southern blot analysis confirmed that the brains of mice with the *Sox1-Cre* allele had lost the floxed *Rest* genes (Fig. 5A). Despite the lack of *Rest* throughout the entire brain tissue (Fig. 5A), brain weight at 8 weeks of age was not significantly different between the mice with and without the *Sox1-Cre* allele (Fig. 5B).

Next, we examined the histology of the brains of mice with and without the *Sox1-Cre* allele at different developmental stages and ages (E16.5, P0, P4, P7, P10, 4 weeks, 8 weeks, 10 weeks, 6 months and 9 months of age). However, we did not find any histological differences in the brains, including in the subgranular zone (SGZ) of the hippocampal dentate gyrus and the subventricular zone (SVZ), where NSCs and NPCs reside and generate new neurons and glia (Fig. 5C) (Gage, 2002). We further performed immunohistochemical staining to examine the expression of various markers, including Prox1, Dcx, RC2, Tuj1, NeuN (Rbfox3 – Mouse Genome Informatics), nestin and Gfap at various time points (E16.5, P4, 8 weeks and 6 months) in the *Rest*-deficient and control brains. Prox1, Dcx and RC2 were used as markers for intermediate progenitor cells, immature neuronal cells and radial glial cells, respectively (Gao et al., 2011; Misson et al., 1988). Importantly, we did not observe any difference in the staining patterns of these markers between *Rest*-deficient and control brains (Fig. 6). We also confirmed that nestin-positive cells and Gfap-positive cells did not express Tuj1 in *Rest*-deficient brain, suggesting that misexpression of Tuj1 does not occur in the *Rest*-deficient cells in vivo (supplementary material Figs S10, S11). Although a recent study showed that acute *Rest* ablation in mice leads to a decreased number of Prox1-positive cells at SGZ regions, we did not observe any significant differences in the number of Prox1-positive cells, even in 9-month-old mice (supplementary material Fig. S12).

In order to examine the effect of *Rest* ablation on the maintenance of adult NSCs, we compared the numbers of BrdU-labeled cells in the SVZ of the adult brain of the *Rest* conditional KO mice carrying the *Sox1-Cre* allele with those of control littermates (Doetsch et al., 2002; Lendahl et al., 1990). BrdU was administered as a daily intraperitoneal injection of 50 mg/kg body weight for 12 days starting at the age of 8 weeks, and the brains were fixed 1 day after the last injection as described previously (Shi et al., 2004). We did not find any significant difference in the number of BrdU-positive cells in the SVZ of these mice (Fig. 7A). We also confirmed co-localization of BrdU-positive cells and those positive for Dcx, a marker for premature neuronal cells, in the SVZ of *Rest*-deficient mice (Fig. 7B), suggesting that adult neurogenesis occurs in these mice. In addition, the localization and the number of differentiated NeuN-positive cells in the adult mouse brain did not differ in the presence or absence of the intact *Rest* gene (Fig.

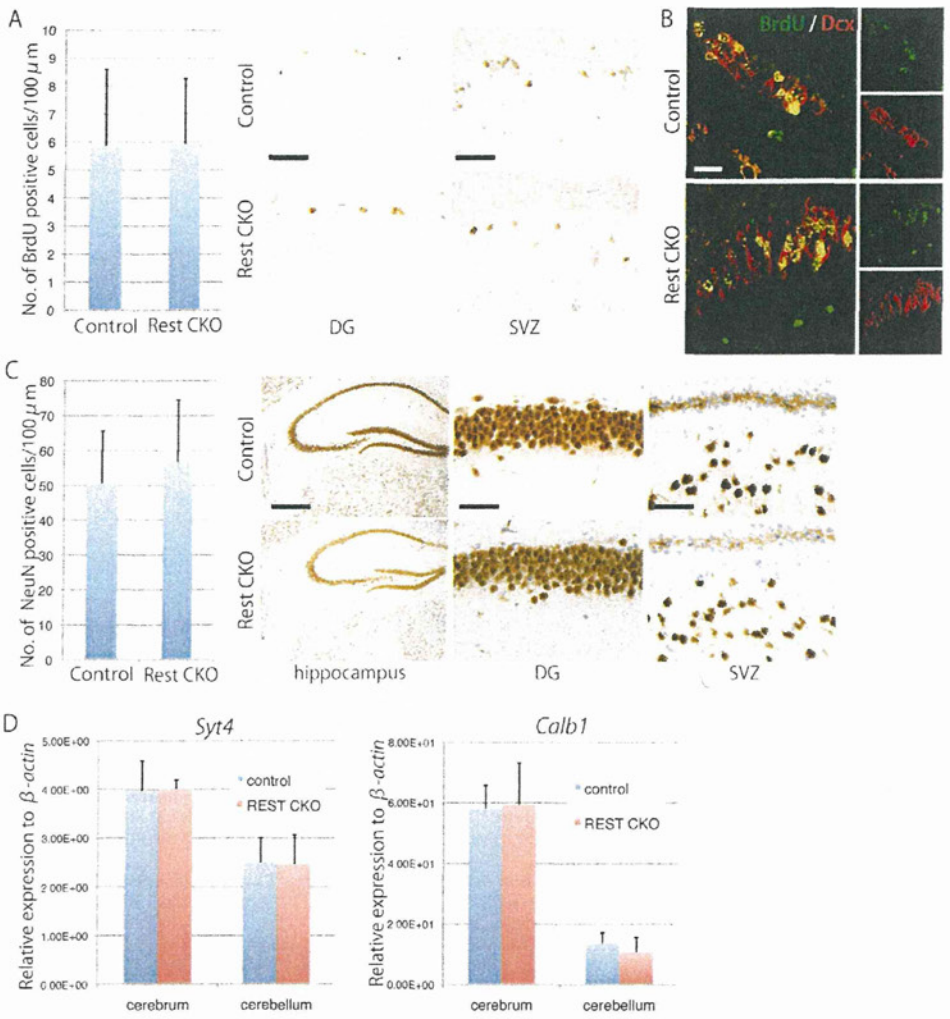

Fig. 7. Adult neurogenesis in *Rest*-deficient brains in vivo. (**A**) Immunohistochemical analysis of BrdU-positive proliferating cells in the adult brain (10 weeks of age). There were no differences in the distribution of BrdU-positive cells in DG and SVZ regardless of genotype. The number of BrdU-positive cells/length of cerebral ventricle in the brains of *Sox1-Cre/+*; *Rest*$^{2lox/2lox}$ mice was not altered compared with that of their control littermates. (**B**) Immunohistochemical staining for BrdU (green) and Dcx (red) double-positive cells in the SVZ of brain from *Sox1-Cre/+*; *Rest*$^{2lox/2lox}$ mice and control littermates at 10 weeks of age. (**C**) Immunohistochemical staining for NeuN in the DG of the hippocampus and SVZ of brains from *Sox1-Cre/+*; *Rest*$^{2lox/2lox}$ mice and their control littermates at 8 weeks of age. (**D**) The expression of Rest target genes in the adult mouse brain at 8 weeks of age. The expression of *Syt4* and *Calb1* was unchanged in the cerebrum and cerebellum of *Sox1-Cre/+*; *Rest*$^{2lox/2lox}$ mice. Transcript levels were normalized to β-actin levels. The data are presented as average values with s.d. of six independent samples. Scale bars: 50 μm in DG and SVZ; 500 μm in hippocampus; 20 μm in B.

7C). A real-time RT-PCR analysis revealed that the expression of *Syt4* and *Calb1* was not altered in the adult brains lacking the CoRest binding site of *Rest* (Fig. 7D).

These results indicate that *Rest* is not required for brain development and suggest that genetic ablation of *Rest* during the initial stage of neural development does not cause any detectable abnormality in adult neurogenesis in vivo.

DISCUSSION

Differentiation of neuronal progenitors to mature neurons proceeds with loss of the Rest repressor complex from the RE1 site of neuronal genes, which is accompanied by increased expression of the target genes (Ballas et al., 2005). In the present study, using *Rest* conditional KO mice we confirmed that *Rest* plays a role in the repression of Rest neuronal target genes in in vitro cultured neuronal progenitor cells to inhibit terminal differentiation. By contrast, genetic ablation of *Rest* in the whole brain in vivo does not result in altered expression of target genes. Furthermore, mice lacking *Rest* in the brain are apparently normal and grow into adults. These findings suggest that, in contrast to the repressive role of *Rest* in in vitro cultured neuronal cells, *Rest* is dispensable for embryonic neurogenesis in vivo.

The unsolved question is why derepression of Rest target genes after *Rest* ablation can be detected in in vitro cultured neuronal cells but not in developing brain tissue in vivo. It has been demonstrated that neuronal progenitor cells are competent for extrinsic signals involved in the specification of cell fate during neurogenesis (Edlund and Jessell, 1999). Our findings suggest that the local environment in the brain, which consists of multiple cell types, is likely to provide complementary regulatory mechanisms for the proper intrinsic regulation of neuronal genes in vivo. It is noteworthy that, in the non-neuronal cells outside of the brain, the derepression of Rest target genes was observed not only in vitro but also in vivo. These findings suggest that the brain-specific environment is important for the complementary repression of Rest target genes in the absence of *Rest*.

Epigenetic mechanisms serve as important interfaces between gene expression and the environment (Jaenisch and Bird, 2003). Given that Rest exerts its repressive effects in conjunction with epigenetic modifiers (Ballas et al., 2005; Naruse et al., 1999; You et al., 2001), it is possible that extrinsic niche signals in the brain compensate for the lack of Rest through epigenetic regulatory mechanisms. Consistent with this hypothesis, we could not detect

any differences in the staining pattern of histone H3K27me3, a mark of epigenetic silencing, between *Rest* wild-type and *Rest*-deficient brains in vivo (data not shown).

Another study indicated that MeCP2 and other co-repressors remained on the Rest target promoters even after loss of Rest from the RE1 site, suggesting that Rest co-repressors might be involved in the additional regulatory mechanisms that are responsible for repressing the expression of neuronal genes in neuronal cells in the absence of Rest (Ballas et al., 2005). It is possible that such factors specifically compensate for the effect of *Rest* ablation in the repression of Rest neuronal target genes during embryonic neurogenesis in vivo. It is also possible that transcriptional activators might be required for the derepression of Rest target genes in the developing brain. In this context, the decreased levels of transcriptional activation might maintain the proper expression levels of Rest target genes in *Rest*-deficient brains in vivo.

A recent study by Gao et al. demonstrated that the acute deletion of *Rest* in the adult dentate gyrus (DG) leads to a decreased number of Prox1-positive DG cells (Gao et al., 2011). However, in the present study, we did not observe any significant differences in the number of Prox1-positive DG cells upon *Rest* ablation, even in 9-month-old mice. A possible explanation for the discrepancy is that the acute deletion of *Rest* in the adult DG cannot activate the compensatory mechanisms, resulting in premature differentiation of adult NSCs, whereas its deletion at the early embryonic stage, as performed in this experiment, activates the complementary machinery that masks Rest function at adult stages. Therefore, further experiments are still required to determine the role of Rest in the maintenance of adult NSCs in vivo.

The expression of Rest target genes in MEFs/TTFs is upregulated upon the loss of *Rest*, suggesting that Rest is involved in the active repression of neuronal genes in non-neuronal cells outside of the brain. However, we found that *Bdnf*, which contains RE1 sites and is repressed by Rest in ESCs (Yamada et al., 2010), was not derepressed after the deletion of *Rest* in MEFs/TTFs. As reported in a previous study (Chen et al., 1998), these findings suggest that there is cell type specificity of Rest-mediated gene silencing. In addition, a microarray analysis revealed that only a subset of genes with a Rest binding site (27%) is derepressed by more than 2-fold following genetic ablation of *Rest* in non-neuronal tissues. In addition to the cell type-specific repression, these findings suggest that there is gene-specific repression by Rest (Chen et al., 1998). Since epigenetic silencing occurs through multiple modifications, including DNA methylation and histone modifications (Jaenisch and Bird, 2003; Lunyak et al., 2002; Martinowich et al., 2003), *Rest* deletion alone might not be sufficient to reactivate the silenced locus once silencing, involving multiple epigenetic modifications, has been completed. It is also possible that the cell type- and gene-specific activity of transcriptional activators is responsible for such different responses to *Rest* deletion.

The impaired interaction of Rest with its target genes has been reported in various neurological and neurodegenerative diseases. Although we found that mice lacking the CoRest binding site of *Rest* in the brain had no gross anatomical abnormalities even upon reaching adulthood, it is possible that more detailed analyses might highlight behavioral abnormalities in the *Rest* KO mice. In this context, these mice might be useful in investigation of the role of altered Rest interactions in neurological and neurodegenerative diseases. It would also be interesting to examine the functional alterations of *Rest*-deficient neuronal cells in vivo, which eventually might uncover the pathogenesis of such diseases.

In summary, we have generated *Rest* conditional KO mice and examined the effects of *Rest* ablation in neuronal and non-neuronal cells in vitro and in vivo. We showed that, in contrast to the role of *Rest* in the repression of Rest target genes in in vitro cultured neuronal cells, as well as in non-neuronal cells outside of the brain, the CoRest binding site of *Rest* is dispensable for embryonic neurogenesis in vivo.

Acknowledgements

We thank Kyoko Takahashi and Ayako Suga for technical assistance; Caroline Beard for the *Col1a-tetOP-cre* allele; and Shinichi Nishikawa for *Sox1-Cre* mice.

Funding

This study was supported by grants from the Ministry of Education, Culture, Sports, Science and Technology of Japan; Precursory Research for Embryonic Science and Technology (PRESTO); and the Ministry of Health, Labour and Welfare of Japan.

Competing interests statement

The authors declare no competing financial interests.

Supplementary material

Supplementary material available online at
http://dev.biologists.org/lookup/suppl/doi:10.1242/dev.072272/-/DC1

References

Abrajano, J. J., Qureshi, I. A., Gokhan, S., Zheng, D., Bergman, A. and Mehler, M. F. (2009). Differential deployment of REST and CoREST promotes glial subtype specification and oligodendrocyte lineage maturation. *PLoS ONE* **4**, e7665.

Andres, M. E., Burger, C., Peral-Rubio, M. J., Battaglioli, E., Anderson, M. E., Grimes, J., Dallman, J., Ballas, N. and Mandel, G. (1999). CoREST: a functional corepressor required for regulation of neural-specific gene expression. *Proc. Natl. Acad. Sci. USA* **96**, 9873-9878.

Ballas, N., Battaglioli, E., Atouf, F., Andres, M. E., Chenoweth, J., Anderson, M. E., Burger, C., Moniwa, M., Davie, J. R., Bowers, W. J. et al. (2001). Regulation of neuronal traits by a novel transcriptional complex. *Neuron* **31**, 353-365.

Ballas, N., Grunseich, C., Lu, D. D., Speh, J. C. and Mandel, G. (2005). REST and its corepressors mediate plasticity of neuronal gene chromatin throughout neurogenesis. *Cell* **121**, 645-657.

Bassuk, A. G., Wallace, R. H., Buhr, A., Buller, A. R., Afawi, Z., Shimojo, M., Miyata, S., Chen, S., Gonzalez-Alegre, P., Griesbach, H. L. et al. (2008). A homozygous mutation in human PRICKLE1 causes an autosomal-recessive progressive myoclonus epilepsy-ataxia syndrome. *Am. J. Hum. Genet.* **83**, 572-581.

Beard, C., Hochedlinger, K., Plath, K., Wutz, A. and Jaenisch, R. (2006). Efficient method to generate single-copy transgenic mice by site-specific integration in embryonic stem cells. *Genesis* **44**, 23-28.

Bruce, A. W., Donaldson, I. J., Wood, I. C., Yerbury, S. A., Sadowski, M. I., Chapman, M., Gottgens, B. and Buckley, N. J. (2004). Genome-wide analysis of repressor element 1 silencing transcription factor/neuron-restrictive silencing factor (REST/NRSF) target genes. *Proc. Natl. Acad. Sci. USA* **101**, 10458-10463.

Canzonetta, C., Mulligan, C., Deutsch, S., Ruf, S., O'Doherty, A., Lyle, R., Borel, C., Lin-Marq, N., Delom, F., Groet, J. et al. (2008). DYRK1A-dosage imbalance perturbs NRSF/REST levels, deregulating pluripotency and embryonic stem cell fate in Down syndrome. *Am. J. Hum. Genet.* **83**, 388-400.

Chen, Z. F., Paquette, A. J. and Anderson, D. J. (1998). NRSF/REST is required in vivo for repression of multiple neuronal target genes during embryogenesis. *Nat. Genet.* **20**, 136-142.

Chong, J. A., Tapia-Ramirez, J., Kim, S., Toledo-Aral, J. J., Zheng, Y., Boutros, M. C., Altshuller, Y. M., Frohman, M. A., Kraner, S. D. and Mandel, G. (1995). REST: a mammalian silencer protein that restricts sodium channel gene expression to neurons. *Cell* **80**, 949-957.

Doetsch, F., Petreanu, L., Caille, I., Garcia-Verdugo, J. M. and Alvarez-Buylla, A. (2002). EGF converts transit-amplifying neurogenic precursors in the adult brain into multipotent stem cells. *Neuron* **36**, 1021-1034.

Edlund, T. and Jessell, T. M. (1999). Progression from extrinsic to intrinsic signaling in cell fate specification: a view from the nervous system. *Cell* **96**, 211-224.

Fink, T. L., Francis, S. H., Beasley, A., Grimes, K. A. and Corbin, J. D. (1999). Expression of an active, monomeric catalytic domain of the cGMP-binding cGMP-specific phosphodiesterase (PDE5). *J. Biol. Chem.* **274**, 34613-34620.

Gage, F. H. (2002). Neurogenesis in the adult brain. *J. Neurosci.* **22**, 612-613.

Gao, Z., Ure, K., Ding, P., Nashaat, M., Yuan, L., Ma, J., Hammer, R. E. and Hsieh, J. (2011). The master negative regulator REST/NRSF controls adult

neurogenesis by restraining the neurogenic program in quiescent stem cells. *J. Neurosci.* **31**, 9772-9786.
Hatano, Y., Yamada, Y., Hata, K., Phutthaphadoong, S., Aoki, H. and Hara, A. (2011). Genetic ablation of a candidate tumor suppressor gene, Rest, does not promote mouse colon carcinogenesis. *Cancer Sci.* **102**, 1659-1664.
Hochedlinger, K., Yamada, Y., Beard, C. and Jaenisch, R. (2005). Ectopic expression of Oct-4 blocks progenitor-cell differentiation and causes dysplasia in epithelial tissues. *Cell* **121**, 465-477.
Jaenisch, R. and Bird, A. (2003). Epigenetic regulation of gene expression: how the genome integrates intrinsic and environmental signals. *Nat. Genet.* **33 Suppl.**, 245-254.
Jepsen, K., Hermanson, O., Onami, T. M., Gleiberman, A. S., Lunyak, V., McEvilly, R. J., Kurokawa, R., Kumar, V., Liu, F., Seto, E. et al. (2000). Combinatorial roles of the nuclear receptor corepressor in transcription and development. *Cell* **102**, 753-763.
Johnson, R., Gamblin, R. J., Ooi, L., Bruce, A. W., Donaldson, I. J., Westhead, D. R., Wood, I. C., Jackson, R. M. and Buckley, N. J. (2006). Identification of the REST regulon reveals extensive transposable element-mediated binding site duplication. *Nucleic Acids Res.* **34**, 3862-3877.
Johnson, R., Teh, C. H., Kunarso, G., Wong, K. Y., Srinivasan, G., Cooper, M. L., Volta, M., Chan, S. S., Lipovich, L., Pollard, S. M. et al. (2008). REST regulates distinct transcriptional networks in embryonic and neural stem cells. *PLoS Biol.* **6**, e256.
Kohyama, J., Sanosaka, T., Tokunaga, A., Takatsuka, E., Tsujimura, K., Okano, H. and Nakashima, K. (2010). BMP-induced REST regulates the establishment and maintenance of astrocytic identity. *J. Cell Biol.* **189**, 159-170.
Lendahl, U., Zimmerman, L. B. and McKay, R. D. (1990). CNS stem cells express a new class of intermediate filament protein. *Cell* **60**, 585-595.
Lepagnol-Bestel, A. M., Zvara, A., Maussion, G., Quignon, F., Ngimbous, B., Ramoz, N., Imbeaud, S., Loe-Mie, Y., Benihoud, K., Agier, N. et al. (2009). DYRK1A interacts with the REST/NRSF-SWI/SNF chromatin remodelling complex to deregulate gene clusters involved in the neuronal phenotypic traits of Down syndrome. *Hum. Mol. Genet.* **18**, 1405-1414.
Lunyak, V. V., Burgess, R., Prefontaine, G. G., Nelson, C., Sze, S. H., Chenoweth, J., Schwartz, P., Pevzner, P. A., Glass, C., Mandel, G. et al. (2002). Corepressor-dependent silencing of chromosomal regions encoding neuronal genes. *Science* **298**, 1747-1752.
Martinowich, K., Hattori, D., Wu, H., Fouse, S., He, F., Hu, Y., Fan, G. and Sun, Y. E. (2003). DNA methylation-related chromatin remodeling in activity-dependent BDNF gene regulation. *Science* **302**, 890-893.
Misson, J. P., Edwards, M. A., Yamamoto, M. and Caviness, V. S., Jr (1988). Identification of radial glial cells within the developing murine central nervous system: studies based upon a new immunohistochemical marker. *Brain Res. Dev. Brain Res.* **44**, 95-108.
Naruse, Y., Aoki, T., Kojima, T. and Mori, N. (1999). Neural restrictive silencer factor recruits mSin3 and histone deacetylase complex to repress neuron-specific target genes. *Proc. Natl. Acad. Sci. USA* **96**, 13691-13696.
Otto, S. J., McCorkle, S. R., Hover, J., Conaco, C., Han, J. J., Impey, S., Yochum, G. S., Dunn, J. J., Goodman, R. H. and Mandel, G. (2007). A new binding motif for the transcriptional repressor REST uncovers large gene networks devoted to neuronal functions. *J. Neurosci.* **27**, 6729-6739.
Pevny, L. H., Sockanathan, S., Placzek, M. and Lovell-Badge, R. (1998). A role for SOX1 in neural determination. *Development* **125**, 1967-1978.
Roopra, A., Qazi, R., Schoenike, B., Daley, T. J. and Morrison, J. F. (2004). Localized domains of G9a-mediated histone methylation are required for silencing of neuronal genes. *Mol. Cell* **14**, 727-738.
Schoenherr, C. J. and Anderson, D. J. (1995). The neuron-restrictive silencer factor (NRSF): a coordinate repressor of multiple neuron-specific genes. *Science* **267**, 1360-1363.
Schoenherr, C. J., Paquette, A. J. and Anderson, D. J. (1996). Identification of potential target genes for the neuron-restrictive silencer factor. *Proc. Natl. Acad. Sci. USA* **93**, 9881-9886.
Shi, Y., Sawada, J., Sui, G., Affar, El B., Whetstine, J. R., Lan, F., Ogawa, H., Luke, M. P. and Nakatani, Y. (2003). Coordinated histone modifications mediated by a CtBP co-repressor complex. *Nature* **422**, 735-738.
Shi, Y., Chichung Lie, D., Taupin, P., Nakashima, K., Ray, J., Yu, R. T., Gage, F. H. and Evans, R. M. (2004). Expression and function of orphan nuclear receptor TLX in adult neural stem cells. *Nature* **427**, 78-83.
Strutz, F., Okada, H., Lo, C. W., Danoff, T., Carone, R. L., Tomaszewski, J. E. and Neilson, E. G. (1995). Identification and characterization of a fibroblast marker: FSP1. *J. Cell Biol.* **130**, 393-405.
Takashima, Y., Era, T., Nakao, K., Kondo, S., Kasuga, M., Smith, A. G. and Nishikawa, S. (2007). Neuroepithelial cells supply an initial transient wave of MSC differentiation. *Cell* **129**, 1377-1388.
Tapia-Ramirez, J., Eggen, B. J., Peral-Rubio, M. J., Toledo-Aral, J. J. and Mandel, G. (1997). A single zinc finger motif in the silencing factor REST represses the neural-specific type II sodium channel promoter. *Proc. Natl. Acad. Sci. USA* **94**, 1177-1182.
Vierbuchen, T., Ostermeier, A., Pang, Z. P., Kokubu, Y., Sudhof, T. C. and Wernig, M. (2010). Direct conversion of fibroblasts to functional neurons by defined factors. *Nature* **463**, 1035-1041.
Yamada, Y., Aoki, H., Kunisada, T. and Hara, A. (2010). Rest promotes the early differentiation of mouse ESCs but is not required for their maintenance. *Cell Stem Cell* **6**, 10-15.
You, A., Tong, J. K., Grozinger, C. M. and Schreiber, S. L. (2001). CoREST is an integral component of the CoREST- human histone deacetylase complex. *Proc. Natl. Acad. Sci. USA* **98**, 1454-1458.
Zuccato, C., Belyaev, N., Conforti, P., Ooi, L., Tartari, M., Papadimou, E., MacDonald, M., Fossale, E., Zeitlin, S., Buckley, N. et al. (2007). Widespread disruption of repressor element-1 silencing transcription factor/neuron-restrictive silencer factor occupancy at its target genes in Huntington's disease. *J. Neurosci.* **27**, 6972-6983.

Cancer Science
The official journal of the Japanese Cancer Association JCA

Genetic ablation of a candidate tumor suppressor gene, *Rest*, does not promote mouse colon carcinogenesis

Yuichiro Hatano,[1] Yasuhiro Yamada,[2,3,5] Kazuya Hata,[1] Suphot Phutthaphadoong,[1] Hitomi Aoki[4] and Akira Hara[1]

[1]Department of Tumor Pathology, Gifu University Graduate School of Medicine, Gifu; [2]PRESTO, Japan Science and Technology Agency, Saitama; [3]Center for iPS Cell Research and Application, Institute for Integrated Cell-Material Sciences, Kyoto University, Kyoto; [4]Department of Tissue and Organ Development, Gifu University Graduate School of Medicine, Gifu, Japan

(Received March 23, 2011/Revised May 30, 2011/Accepted June 7, 2011/Accepted manuscript online June 11, 2011/Article first published online July 21, 2011)

Colon carcinogenesis is a multistage process involving genetic alterations of various tumor suppressor genes and oncogenes. Repressor element 1 silencing factor (*REST*), which was originally discovered as a transcriptional repressor of neuronal genes, plays an important role in neuronal differentiation. In a previous genetic screening for tumor suppressor genes in human cancers, *REST* was identified as a candidate tumor suppressor gene in colorectal carcinogenesis. However, the role of *Rest* in colon carcinogenesis *in vivo* remains unclear because of the embryonic lethal phenotype of the conventional *Rest* knockout mouse. In the present study, we conditionally deleted the *Rest* gene in the intestinal epithelium and investigated the effect of *Rest* ablation in mouse colon tumorigenesis. A conditional ablation of *Rest* in the colonic crypts led to a rapid upregulation of Rest-targeted genes, such as *Syt4*, *Bdnf*, and *Tubb3*, suggesting that Rest actually suppresses the expression of its target genes in the colon. However, *Rest* ablation did not lead to any significant effect on the development of colon tumors in two independent mouse models of colon carcinogenesis. In addition, despite the upregulation of neuronal genes in the colonic crypts, no neuronal differentiation was observed in the colonic crypts and tumors after the *Rest* ablation. These results indicate that the loss of *Rest* expression by itself does not promote the development of colon tumors in mice, and suggest that REST may exert a tumor suppressing activity in conjunction with the additional genetic/epigenetic abnormalities that occur during colon carcinogenesis. (*Cancer Sci* 2011; 102: 1659–1664)

Repressor element 1 silencing factor (REST; also called neuron-restrictive silencing factor [NRSF]) was originally discovered as a transcriptional repressor of a number of neuronal genes.[1,2] REST binds to a conserved 21–23 bp motif known as repressor element 1 within the control regions of target genes, and recruits multiple co-factors through repressor domains to alter epigenetic modifications, leading to the generation of a silencing complex. REST is ubiquitously expressed in non-neuronal cells,[3] and it prevents neuronal gene expression in non-neuronal cells.[4]

A link between *REST* dysfunction and carcinogenesis has been recognized[5–7] in a number of cancers such as prostate cancer,[8] breast cancer,[9–11] small cell lung cancer,[12–16] medulloblastoma,[17–19] and neuroblastoma.[20–23] In an RNAi-based screening for tumor suppressor genes, *REST* was identified as a candidate novel tumor suppressor gene.[24] Consistent with this notion, a *REST* mutation was identified in a colon cancer cell line, DLD-1, and the *REST* locus is deleted in approximately one-third of human colon cancers (14 of 42 primary tumors and 13 of 38 cell lines).[24] In addition, exogenous *REST* has been shown to suppress the growth of the colon cancer cells that lack *REST* expression, suggesting that REST actually plays a role in the tumor suppression *in vitro*. Although REST-mediated cellular transformation is proposed to be associated with the PI3K pathway, the precise mechanism(s) underlying the involvement of *REST* in colon carcinogenesis remain unclear. In particular, there is no *in vivo* evidence that establishes the function of *Rest* in tumor suppression.

In the present study, we examined the effect of genetic ablation of *Rest* during colon carcinogenesis *in vivo*. We herein show that genetic deletion of *Rest* results in derepression of the Rest-targeted neuronal genes in the colonic crypts, however, *Rest* ablation does not promote mouse colon carcinogenesis.

Materials and Methods

Animals. All animal experiments were approved by the Animal Research Committee of the Graduate School of Medicine, Gifu University (Gifu, Japan). In a previous study, homozygous *Rest* knockout (KO) mice showed embryonic lethality around E10.5, with a growth retardation phenotype.[25] In the present study, in order to investigate the effect of *Rest* deletion on colon carcinogenesis *in vivo*, we used mice expressing conditional knockout alleles of *Rest*.[26] In the *Rest* conditional mice, the endogenous *Rest* loci were replaced by the conditional KO alleles carrying the floxed last exon, which encodes the CoRest binding site that is essential for the generation of the silencing complex.[27] An *ires-Gfp* sequence was inserted into the 3′-UTR of the *Rest* gene to monitor the transcription of the modified allele ($Rest^{2lox}$ allele). The $Rest^{2lox}$ allele was recombined into the $Rest^{1lox}$ allele in the presence of Cre recombinase. Despite the presence of the remaining exons 1–3 of the $Rest^{1lox}$ allele, altered *Rest* transcripts were not detected in $Rest^{1lox/1lox}$ mouse embryonic stem cells,[26] thus suggesting the 1lox allele to be equivalent to the conventional KO allele.

$Apc^{Min/+}$ mice, doxycycline-inducible *Cre* mice, and intestinal epithelium-specific *Cre*-expressing (*Fabp-Cre*) mice were described previously.[26,28,29] Doxycycline-inducible *Cre* mice harbor two transgenes, *Rosa26-M2rtTA* and *Col1A1-tetO-Cre*.[26] The experimental mice were obtained by breeding.

Experimental procedures. We tested the effect of *Rest* ablation in mouse colon carcinogenesis in two independent experiments (Fig. 1). The first experiment (protocol 1) was a chemically-induced colon carcinogenesis model using doxycycline-inducible *Cre*-expressing mice. The other experiment (protocol 2) used the $Apc^{Min/+}$ mouse colon carcinogenesis model combined with the *Fabp-Cre* mouse. In protocol 1, Cre recombinase was induced by doxycycline treatment after carcinogen exposure, mimicking when the *Rest* gene is lost after the initiation phase of carcinogenesis. In contrast, in protocol 2,

[5]To whom correspondence should be addressed.
E-mail: y-yamada@cira.kyoto-u.ac.jp

doi: 10.1111/j.1349-7006.2011.02006.x